

Radiation Grafted Membranes

Selmiye Alkan Gürsel^{1,3} · Lorenz Gubler¹ (✉) · Bhuvanesh Gupta² ·
Günther G. Scherer¹

¹Electrochemistry Laboratory, Paul Scherrer Institut, 5232 Villigen PSI, Switzerland
lorenz.gubler@psi.ch

²Department of Textile Technology, Indian Institute of Technology, 110016 New Delhi,
India

³*Present address:*

Faculty of Engineering and Natural Sciences, Sabanci University, 34956 Tuzla/Istanbul,
Turkey

1	Introduction	3
2	Preparation of Radiation Grafted Membranes	4
2.1	Nature of Radiation	5
2.2	Graft Polymerization	6
2.3	Radiation Effects on Polymers	8
2.4	Grafting Parameters	11
2.4.1	Nature of Base Polymer	13
2.4.2	Irradiation Dose and Dose Rate	15
2.4.3	Monomer Concentration	18
2.4.4	Grafting Temperature	20
2.4.5	Grafting Medium	21
2.4.6	Additives	24
2.5	Crosslinking	24
2.6	Sulfonation	28
3	Characterization and Structure of Grafted Films and Membranes	29
3.1	Graft Mapping	29
3.2	Surface Chemistry and Surface Morphology	32
3.3	Thermal Characterization	36
3.4	Mechanical Properties	39
4	Fuel Cell Application	40
4.1	Membrane Properties Relevant to Fuel Cell Application	40
4.1.1	Ion Exchange Capacity	41
4.1.2	Water Uptake	43
4.1.3	Conductivity	45
4.2	Performance in Fuel Cells	47
4.2.1	MEA Fabrication	48
4.2.2	Fuel Cell Testing	48
4.2.3	Water States and Water Management	48
4.2.4	Reactant Permeability	50
4.2.5	Chemical Stability	50
4.2.6	Mechanical Integrity	51

52	4.2.7 Fuel Cell Performance	51	52
53	4.2.8 Performance in Direct Methanol Fuel Cells	53	53
54			54
55	5 Conclusions	54	55
56			56
57	References	55	57
58			58

59 **Abstract** The development of proton-exchange membranes for fuel cells has generated 59
60 global interest in order to have a potential source of power for stationary and portable 60
61 applications. The membrane is the heart of a fuel cell and the performance of a fuel cell 61
62 depends largely on the physico-chemical nature of the membrane and its stability in the 62
63 hostile environment of hydrogen and oxygen at elevated temperatures. Efforts are being 63
64 made to develop membranes that are similar to commercial Nafion membranes in 64
65 performance and are available at an affordable price. The radiation grafting of styrene 65
66 and its derivatives onto existing polymer films and subsequent sulfonation of the grafted 66
67 films has been an attractive route for developing these membranes with required chem- 67
68 istry and properties. The process of radiation grafting offers enormous possibilities for 68
69 design of the polymer architecture by careful variation of the irradiation and the graft- 69
70 ing conditions. A wide range of crosslinkers are available, which introduce stability to the 70
71 membrane during its operation in fuel cells. Crosslinking of the base polymer prior to 71
72 grafting has also been an attractive means of obtaining membranes with better perform- 72
73 ance. A systematic presentation is made of the grafting process into different polymers, 73
74 the physical properties of the resultant membranes, and the fuel cell application of these 74
75 membranes. 75

76 **Keywords** Polymer electrolyte fuel cell · Proton exchange membrane · Radiation grafting 77
78 78
79 79

80 Abbreviations 80

81	ATR	Attenuated total reflection spectroscopy	81
82	c_{H^+}	Volumetric density of protons	82
83	DG	Degree of grafting	83
84	D_{H^+}	Proton diffusion coefficient	84
85	DSC	Differential scanning calorimetry	85
86	DVB	Divinylbenzene	86
87	ESR	Electron spin resonance	87
88	ETFE	Poly(ethylene- <i>alt</i> -tetrafluoroethylene)	88
89	FEP	Poly(tetrafluoroethylene- <i>co</i> -hexafluoropropylene)	89
90	FTIR	Fourier transform infrared spectroscopy	90
91	G value	Radiation chemical yield	91
92	Gy	Gray	92
93	IEC	Ion exchange capacity	93
94	MEA	Membrane electrode assembly	94
95	MFI	Melt flow index	95
96	m	Mass	96
97	$n(H_2O)$	Number of water molecules	97
98	$n(SO_3H)$	Number of exchange sites	98
99	PEFC	Polymer electrolyte fuel cell	99
100	PFA	Poly(tetrafluoroethylene- <i>co</i> -perfluorovinyl ether)	100
101	pK_a	Acid dissociation constant	101
102			102

103	PSSA	Polystyrene sulfonic acid	103
104	PTFE	Poly(tetrafluoroethylene)	104
105	PVDF	Poly(vinylidene fluoride)	105
106	SANS	Small angle neutron scattering	106
107	SAXS	Small angle X-ray scattering	107
108	SEM	Scanning electron microscopy	108
109	-SO ₃ H	Sulfonic acid	109
110	TAC	Triallylcyanurate	110
111	TFS	α,β,β -Trifluorostyrene	111
112	T_g	Glass transition temperature	112
113	TGA	Thermogravimetric analysis	113
114	T_m	Melting temperature	114
115	XMA	X-ray microprobe analysis	115
116	XPS	X-ray photoelectron spectroscopy	116
117	ϕ	Water uptake	117
118	λ	Hydration number	118
119	σ_{H^+}	Proton conductivity	119

1 Introduction

Membrane science and technology is the fascinating world of polymers, which extends from separation science and bioreactors to environmental care and electrochemistry [1]. The attraction of membranes lies in their energy-efficient processes combined with their low cost separation, as compared to conventional techniques. The versatile nature of membranes has made their application areas grow enormously. Membranes with different shapes and chemical designs are available, which makes them suitable for processes such as nanofiltration, reverse osmosis, pervaporation, bioreactors, dialysis, electrodialysis, electrolysis, and fuel cells. Membranes have generated considerable interest as solid polymer electrolytes in fuel cells, which have been identified as a promising source of power for stationary and portable applications [2]. The fuel cell offers several advantages in terms of the high power densities and having water as a by-product, which makes it an eco-friendly alternative for energy production. The membrane in a fuel cell offers support structure for the electrodes and allows proton transport across its matrix from anode to cathode. The fuel cell requires a proton exchange membrane that shows good mechanical strength, high chemical stability, and appropriate ionic conductivity (e.g., $> 10^{-2}$ S cm⁻¹). In the current state of technology, perfluorinated membrane materials such as Nafion (DuPont, USA), Flemion (Asahi Glass, Japan), and Aciplex (Asahi Kasei, Japan) are used predominantly in polymer electrolyte fuel cells, due to their attractive conductivity and chemical stability. However, for market introduction of fuel cell products, cost-competitive membrane technology has to be developed. The Nafion

membrane, for instance, has shown good performance in fuel cells but has certain limitations, i.e., it has poor ionic conductivity at low humidity and is available at an expensive rate of ~ 500 $\$/\text{m}^2$. The costs for Nafion, for example, become attractive only at high production volumes [3]. Consequently, the search for new membrane materials with low cost and the required electrochemical characteristics, along with performances matching those of Nafion, is continuing and has become the most focused research area in the design of polymer electrolyte fuel cells.

Both the physical and chemical factors are essential for the establishment of a critical relationship between the structure and performance of a membrane in operation. Therefore, designing a membrane needs proper understanding of both the polymeric material and the fuel cell requirements. With no other membrane in sight and under the complexity of inventing new materials, it becomes necessary to modify existing materials into required membrane structures. A great deal of research effort has been directed to the development of membranes by introducing ionic functionality into different polymers. The sulfonation of polymer films such as in polyetheretherketone and polysulfone is one such approach being used to develop ionic membranes [4–6]. However, the ionic character of membranes needs to be accompanied by their good performance in fuel cell application. That is why the current efforts have been directed to the modification of existing polymer films in such a way that the modified material acquires desired functionality and performs well. Although the base matrix may be any type of polymer, the selection of the fluorinated or perfluorinated polymer matrix has been a prime consideration due to the better chemical and thermal resistance that these polymers provide. Consequently, the functionalization of these polymers by radiation grafting of appropriate monomers has become an attractive way to develop such membranes. It is quite spectacular to envisage that polymers can be altered into materials that display a unique combination of characteristics such as ionic nature, water absorption, and high conductivity. Enormous work has been carried out on the graft modification of polymers and several reviews have been published in this domain [7–13]. Recent reviews related to radiation grafting on fluoropolymers provide thorough knowledge in this area [14–20].

We have confined our goal to reviewing the state-of-the-art in the development of radiation grafted proton-exchange membranes. This review provides an up-to-date summary of the synthesis, properties, and applications of radiation grafted membranes as solid polymer electrolytes in fuel cells.

2 Preparation of Radiation Grafted Membranes

A graft copolymer, in general, can be defined as consisting of one or more types of molecules, as block, connected as side chains to a main chain. These

side chains should have constitutional or configurational features that differ from those of the main chain. The modification of polymers through graft polymerization offers an interesting route for achieving membranes with desirable characteristics. Depending on the chemical nature of the monomer, membranes with desired physico-chemical properties may be fabricated. Therefore, if the monomer is ionic in nature, the grafted membrane acquires ionic character with little influence on most of its inherent characteristics. In this section we describe vital aspects that influence membrane fabrication and performance.

2.1 Nature of Radiation

Membrane development requires activation of the entire bulk of the film so that modification across the film may be achieved. This makes it necessary to use high energy radiation, which may penetrate and produce ionization of the polymer matrix. The nature of the radiation has significant impact on the physical and chemical properties of the resultant membrane. A wide range of types of high energy radiation are available to be used for the grafting process. The radiation may be either electromagnetic in nature, such as X-rays and gamma rays, or charged particles, such as beta particles and electrons. The basic difference between the two types of radiation lies in the higher penetration of the electromagnetic radiation. Charged particles lose energy almost continuously through a large number of small energy transfers while passing through matter. However, photons tend to lose a relatively large amount of intensity by interaction with matter. The advantage of electromagnetic radiation, such as gamma rays, is that the fractions of photons that do not interact with a finite thickness of the material are transmitted with their original energies and directions (exponential attenuation law). Hence, the dose rate of radiation may be easily controlled by the use of a suitable attenuator without influencing the photon energy, which is a very important aspect in radiation-initiated polymerization of monomers.

Although different gamma sources are available today, the most versatile gamma radiation source is Co^{60} , which has a long half-life of 5.3 years and emits radiation of 1.17 and 1.33 MeV (mean value of 1.25 MeV). Two different types of gamma radiation source are available for irradiation. One of the sources is a cavity-type unit where a hollow source in the form of a cylinder remains stationary. The Co^{60} remains in this cylindrical structure as the pins. The sample is introduced into this cylinder cavity by means of a moving drawer. The sample moves down inside the cavity during the exposure stage. Once the irradiation is over, the sample is drawn out and may be subsequently removed. The second type of source is a cave-type where Co^{60} is kept in a shielded container. The whole unit is kept underground and the source moves out with the help of a moving belt for irradiation of a station-

ary sample. The latter type is usually used for the irradiation of samples at an industrial scale.

Exposure of the polymer to radiation is expressed as the absorbed dose. The absorbed radiation dose is defined as the amount of energy imparted to the matter. The units initially used for the radiation dose were rad and Mrad. The most recent unit of radiation is Gray (Gy), which corresponds to 10^4 erg g^{-1} . For higher doses, another unit, kilogray (kGy), is used. The dose rate, therefore, is defined as the adsorbed dose per unit time (Gy min^{-1}). Since radiation grafting proceeds by the generation of free radicals on the polymer as well as on the monomer, the G value (i.e., radiation chemical yield, expressed as the number of free radicals generated for 100 eV energy absorbed per gram) plays an important role in the grafting process. For most polymers the G value remains in the range 2–3.

2.2 Graft Polymerization

Radiation-induced grafting is a process where, in a first step, an active site is created in the preexisting polymer. This site is usually a free radical, where the polymer chain behaves like a macroradical. This may subsequently initiate the polymerization of a monomer, leading to the formation of a graft copolymer structure where the backbone is represented by the polymer being modified, and the side chains are formed from the monomer (Fig. 1). This method offers the promise of polymerization of monomers that are difficult to polymerize by conventional methods without residues of initiators and catalysts. Moreover, polymerization can be carried out even at low temperatures, unlike polymerization with catalysts and initiators. Another interesting as-

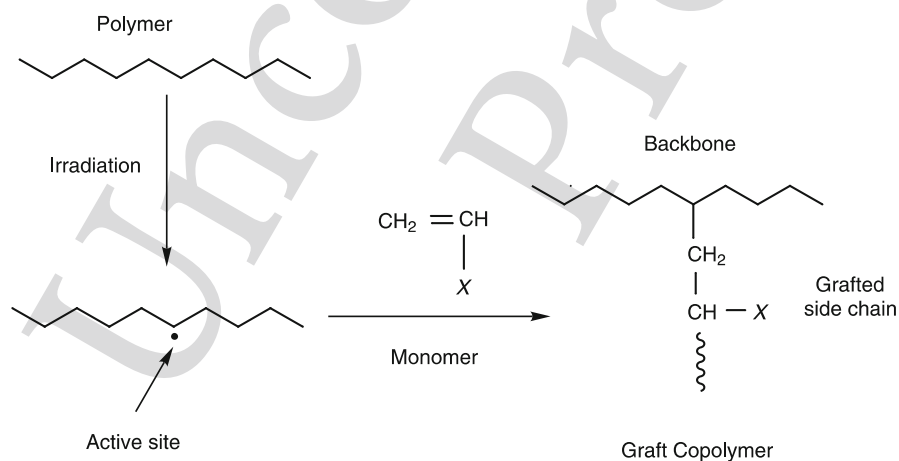


Fig. 1 Radiation-induced grafting

pect of the radiation grafting process is that the grafting may be carried out onto a polymer irrespective of its shape or form. Still, membrane development requires that the grafting is carried out on polymers already existing in the form of a film so that the resultant material remains in sheet form. This overcomes the problem of shaping a grafted polymer bulk into a thin foil. Graft polymerization using high energy radiation is one of the most convenient and the most effective way to develop membranes. By virtue of the high energy of radiation, the photon penetrates effectively into the polymer bulk and activates the matrix thoroughly. This process, therefore, offers a unique way to combine the properties of two highly incompatible polymers. Another attractive feature of radiation grafting is that the degree of grafting may be easily controlled by proper monitoring of the radiation dose, dose rate, and the reaction conditions.

Radiation grafting may be carried out by using three different options [21, 22]:

1. Simultaneous radiation grafting is where both the polymer and the monomer are exposed to radiation. In situ free radical sites are generated and the polymerization of the monomer is initiated. The limitation of this method is that the monomer is continuously exposed to radiation during the grafting reaction and hence extensive homopolymerization proceeds parallel to the grafting reaction, which leads to monomer wastage and a low level of grafting efficiency in a system.
2. Preirradiation grafting (hydroperoxide method) involves activation of the polymer by exposure to radiation under air, which results in the creation of radicals along the macromolecular backbone. These radicals subsequently interact with the oxygen and form peroxides. The graft polymerization is initiated by the decomposition of these peroxides at an elevated temperature. The drawback of this process is that significantly high irradiation doses are needed to achieve a sufficient number of hydroperoxides to accomplish reasonable graft levels, which leads to drastic changes in the physical structure of the polymer and oxidative degradation, even before any grafting is initiated and this is subsequently reflected in the membrane characteristics.
3. Preirradiation grafting (trapped radicals method) involves irradiation of the polymer under inert atmosphere or under vacuum. As a result, the radicals are formed and remain trapped within the polymer matrix. These radicals subsequently initiate the grafting of a monomer.

It is important to mention that because of the inherent differences in the irradiation approaches, the physical characteristics of the membranes will be dependent on the adopted grafting process. The extent of polymerization is expressed as the degree of grafting (DG), which is defined as the percentage mass of the grafted component within the copolymer matrix. On the other

hand, grafting efficiency refers to the percentage conversion of the monomer into the grafted component with respect to the total monomer conversion.

2.3 Radiation Effects on Polymers

Knowledge of the influence of irradiation on polymers is extremely important because even a low irradiation dose may introduce significant alteration in the physical structure of the polymer prior to any grafting being accomplished. The outstanding properties of fluoropolymers, such as excellent chemical resistance, mechanical strength, high temperature stability, and good weathering make them strong candidates as membranes for a highly oxidizing environment such as in fuel cells. However, interaction of the high energy radiation with such polymers may induce significant physical and chemical changes. The irradiation causes ionization of the matrix leading to the formation of ions, radicals, and excited species. The ultimate result is reflected in the chain scission and crosslinking, along with the formation of volatiles, leading to significant variation in the molecular weight of the polymer. The magnitude of these processes will be dependent not only on the chemical nature of the polymer matrix, but also on the nature of the radiation, temperature of the irradiation, and irradiation doses. The irradiation medium may further induce chemical changes depending on the nature of the medium.

Among the fluoropolymers, poly(tetrafluoroethylene) (PTFE) undergoes severe degradation even under mild irradiation conditions both under air and in vacuum [21]. The radiation sensitivity of PTFE is so high that it is readily converted into a low molecular weight fine powder under ionizing radiation. The irradiation leads to the formation of acid fluoride ($-\text{COF}$) groups within the polymer matrix, which easily hydrolyze into carboxylic groups ($-\text{COOH}$) in contact with atmospheric humid air [23, 24]. This is the reason that surface concentration of $-\text{COOH}$ increases with increasing irradiation doses and enhances its surface energy [25]. The polymer degradation is associated with the formation of chain end free radicals, ($-\text{CF}_2-\dot{\text{C}}\text{F}_2$) or chain alkyl radicals, ($-\text{CF}_2-\dot{\text{C}}\text{F}-\text{CF}_2-$), where chain end radicals originate as a result of the main chain scission as observed by electron spin resonance (ESR) [26]. This contributes to the considerable loss in thermal stability of the irradiated polymer and becomes so pronounced that the initial decomposition temperature, as observed in thermogravimetric analysis, is brought down from 530 to 240 °C for an irradiation dose of 100 kGy [27].

The radiation chemistry of copolymers of tetrafluoroethylene with other perfluorinated moieties, such as hexafluoropropylene, is almost identical to that of PTFE with the difference that the relative magnitude of crosslinking and scission varies significantly. The various chemical moieties that have been identified under irradiation are presented in Fig. 2. Although these stud-

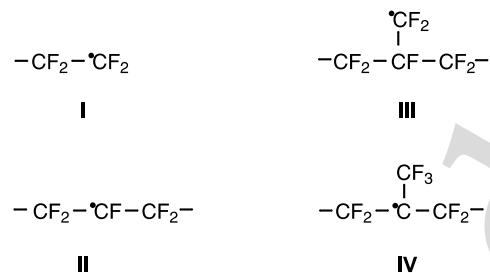


Fig. 2 Possible radicals formed on radiolysis of FEP (redrawn from [30])

ies on radiolysis of poly(tetrafluoroethylene-*co*-hexafluoropropylene) (FEP) are well supported by the studies of Iwasaki et al. [28], there is less agreement on the nature of the radicals and their quantification at different doses [29, 30].

The irradiation temperature of the polymer has distinct influence on the relative proportions of the radical moieties. The irradiation of FEP at a temperature as low as 77 K involves the radicals I and II as the major contributors, while very little originates in the form of III and IV. However, the irradiation at room temperature (300 K) shows a much higher contribution of chain end radicals, with the G values being 0.22 and 2.0 at 77 and 300 K, respectively. As far as the radical concentration in FEP as a function of the irradiation dose at 77 and 300 K is concerned, the radical concentration at 300 K is much higher than at the lower temperature, probably due to the enhanced molecular mobility and resultant chain scission at higher temperature [30]. Identification of the radical I as one of the principal radicals on radiolysis at 77 and 300 K is consistent with the main chain scission being the major bond-breaking step during gamma irradiation of FEP at both these temperatures. These observations are supported by the investigations on poly(tetrafluoroethylene-*co*-perfluorovinyl ether) (PFA). The nature of the radicals in PFA, as determined by ESR, was identified to be I and II. However, G values for radical formation at room temperature and 77 K were found to be 0.93 and 0.16, respectively [31], which is higher than the values for PTFE of 0.4 and 0.14 [32].

There is a systematic difference in the degradation behavior of PTFE from FEP and PFA under ionizing radiation. Both the FEP and PFA contain a pendent group in the form of $-\text{CF}_3$ and $-\text{OC}_3\text{F}_7$, respectively. This has direct bearing on the crystalline structure of the polymer due to impedance in the chain packing by these substituting groups. The higher amorphous region in these two polymers would therefore lead to greater radical mobility and subsequent chain scission as compared to PTFE. The high sensitivity of PTFE to irradiation is because the radicals have restricted movements in a highly crystalline matrix and therefore inhibit radical-radical recombination. Both PFA and FEP undergo side-chain cleavage and therefore have

411 more chain end radicals. Recombination of the radicals is restricted and the
412 chain scission proceeds smoothly, resulting in the formation of a higher num-
413 ber of radicals. This further reflects into the greater number of carboxyl
414 groups (transformation of $-\text{COF}$ to $-\text{COOH}$), which proceeds in the order
415 $\text{FEP} > \text{PFA} > \text{PTFE}$ [33].

416 The irradiation of poly(vinylidene fluoride) (PVDF) brings about little en-
417 hancement in the crystallinity for irradiation doses of about 100 kGy similar
418 to poly(ethylene-*alt*-tetrafluoroethylene) (ETFE). However, beyond 100 kGy,
419 ETFE shows significant loss in the crystallinity but PVDF remains almost un-
420 changed [34].

421 The irradiation of fluoropolymers at elevated temperatures has been ex-
422 plored for the development of materials with better mechanical proper-
423 ties [35]. This arises because of the radiation-induced crosslinking of chains
424 and subsequent higher network density in the resultant polymer [36]. Here,
425 the irradiation is accomplished at a temperature higher than the melting
426 point of the polymer. In the molten state, the polymer behaves as an amorph-
427 ous matrix and the mobility of molecular chains is considerably enhanced.
428 This promotes the mutual recombination of radicals, i.e., crosslinking involv-
429 ing chain end radicals and chain alkyl radicals [37].

430 Irradiation even at a dose as low as 5 kGy brings about a drastic improve-
431 ment in the tensile strength of PTFE. As the irradiation temperature increases
432 from room temperature towards below melting, the mechanical strength de-
433 creases quite rapidly. This is an indication that the chain scission is accel-
434 erated with increasing temperature. However, once the irradiation temperature
435 crosses the melting temperature and reaches beyond 340 °C, both modulus
436 and tensile strength tend to increase considerably, because the polymer enters
437 into a molten state where the network formation is facilitated. Such behavior
438 has been observed by other workers under different irradiation doses [38].
439 It is interesting to note that the crystallinity of the polymer undergoes dras-
440 tic reduction with the increasing dose. This is an obvious outcome of the
441 crosslinking of chains, which lowers the molecular mobility and prevents the
442 chains from undergoing crystallization upon cooling. The crosslinking is so
443 pronounced that an irradiation dose of 2 MGy leads to complete inhibition of
444 crystallization in PTFE [32].

445 The radiation processing of FEP has shown that crosslinking proceeds fa-
446 vorably at temperatures above its glass transition temperature (70–90 °C)
447 under vacuum. The crosslink density, as measured by the gel content, tends to
448 increase sharply upon gamma irradiation at around 90 °C and reaches values
449 as high as 35% at 160 °C [39]. Based on X-ray photoelectron spectroscopy
450 (XPS), it has been found that the radical IV (Fig. 2) dominates over other
451 species under gamma irradiation [40]. This structure originates from the hex-
452 afluoropropylene units in the copolymer. The combination of structure IV
453 with I has been proposed to be the most probable route to the crosslinking
454 reaction. This is further supported by the investigations of Sun et al. [41],

where structure IV was proposed to be the one involved in the crosslinking reaction with other radicals. The tetrafluoroethylene component along the polymer chain still undergoes the crosslinking reaction. Forsythe et al. [42] have made comprehensive studies on the gamma irradiation-induced changes in the chemical and mechanical behavior of poly(tetrafluoroethylene-co-perfluoromethylvinylether). Irradiation at the temperature range 77–195 K did not result in any gel formation, indicating that the crosslinking is almost suppressed at these temperatures. Tensile strength diminished and elongation increased, suggesting that chain scission is the most appropriate change taking place. The strong evidence in favor of this degradation comes from the diminishing glass transition temperature in this temperature range. Crosslinking dominated over chain scission at 263 °C and above, where gelation also approached 80–90% and tensile strength also showed a sharp increase.

2.4 Grafting Parameters

The design of membranes by radiation grafting covers not only the covalently linked incorporation of an ionic component but also requires perfect tailor-making to govern how well the molecular architecture, physical properties, and morphology of the membranes may be controlled. A wide range of polymers have been grafted, predominantly with styrene or its derivatives, using different crosslinkers. Tables 1–3 illustrate the common base films, monomers, and crosslinkers used in radiation-induced grafting [43–46].

Graft polymerization is strongly influenced by irradiation and synthesis conditions, such as radiation dose, dose rate, monomer concentration, reaction temperature, pregrafting storage, solvents, and additives (irrespective of the base matrix). Most of the work on membrane preparation follows the graft polymerization of styrene onto polymers and the subsequent sulfonation. The pioneering work of Chapiro on radiation-induced grafting led to interesting observations on the grafting process and opened up the route for several possibilities in radiochemical grafting of polymer films [47–50]. For most of the polymer–monomer systems, grafting proceeds by the grafting front mechanism, as proposed by Chapiro for grafting into polyethylene and FEP films [51–53]. The initial grafting takes place at the film surface and behaves as the grafting front. This grafted layer swells in the reaction medium and further grafting proceeds by the progressive diffusion of the monomer through this swollen layer and grafting front movement to the middle of the film. This mechanism of grafting has recently been the basis of several other investigations on membrane preparation based on polyethylene, FEP, and PFA films as the base matrix [54–57]. The following sections deal with the various parameters and factors that influence the DG.

Table 1 Common base polymer films used for the preparation of radiation grafted FC membranes [43]

Polymer	Abbreviation	Repeating unit
<i>Perfluorinated polymers</i>		
Polytetrafluoroethylene	PTFE	$\left[\text{CF}_2\text{-CF}_2 \right]_n$
Poly(tetrafluoroethylene-co-hexafluoropropylene)	FEP	$\left[\text{CF}_2\text{-CF}_2 \right]_n \left[\text{CF}_2\text{-CF} \left(\text{CF}_3 \right) \right]_m$
Poly(tetrafluoroethylene-co-perfluoropropyl vinyl ether)	PFA	$\left[\text{CF}_2\text{-CF}_2 \right]_n \left[\text{CF}_2\text{-CF} \left(\text{OC}_3\text{F}_7 \right) \right]_m$
<i>Partially fluorinated polymers</i>		
Polyvinylidene fluoride	PVDF	$\left[\text{CF}_2\text{-CH}_2 \right]_n$
Poly(vinylidene fluoride-co-hexafluoropropylene)	PVDF-co-HFP	$\left[\text{CF}_2\text{-CH}_2 \right]_n \left[\text{CF}_2\text{-CF} \left(\text{CF}_3 \right) \right]_m$
Poly(ethylene-alt-tetrafluoroethylene)	ETFE	$\left[\left(\text{CH}_2\text{-CH}_2 \right) \left(\text{CF}_2\text{-CF}_2 \right) \right]_n$
Polyvinyl fluoride	PVF	$\left[\text{CH}_2\text{-CHF} \right]_n$
<i>Hydrocarbon polymers</i>		
Polyethylene	PE	$\left[\text{CH}_2\text{-CH}_2 \right]_n$

Table 2 Monomers used for the preparation of radiation grafted FC membranes [43]

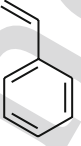
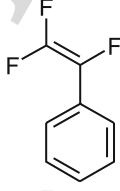
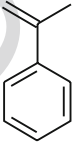
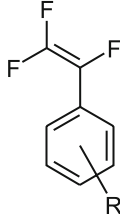
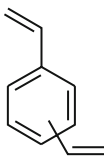
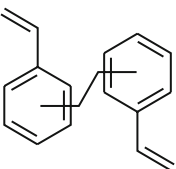
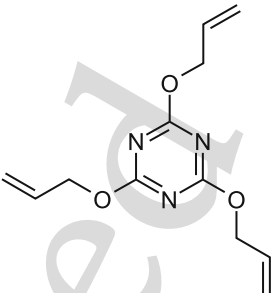
Styrene		α,β,β -Trifluorostyrene (TFS)	
α -Methylstyrene (AMS)		Substituted trifluorostyrene (R = SO ₂ F, Me, MeO, PhO, ...)	

Table 3 Crosslinkers used as comonomers in the radiation grafting process [43]

		
Divinyl benzene (DVB)	Bis(vinyl phenyl)ethane (BVPE)	Triallylcyanurate (TAC)

2.4.1

Nature of Base Polymer

The chemical nature of the base polymer is an important aspect in membrane development. There has been preference for the thermally stable fluorinated polymers over hydrocarbon polymers. Fluorine-containing polymers, characterized by the presence of carbon-fluorine bonds, are widely used as the base matrices owing to their outstanding chemical and thermal stability, low surface energy, and the ease of modification of various properties by the grafting method. Perfluorinated polymers and partially fluorinated polymers combining hydrocarbon and fluorocarbon structures are excellent candidates as base polymers. For instance, fluorinated FEP has drawn wide attention due to its reasonably good radiation stability [58].

The membranes, developed at the Paul Scherer Institut (PSI, Switzerland) for fuel cell applications, were initially based on FEP [59–61]. The use of ETFE as base material was revisited recently in this laboratory since ETFE is readily available in higher molecular weights and has desirable mechanical properties such as breaking strength and flexibility, which are enhanced with increasing molecular weight [62]. ETFE contains alternating structural units of ethylene and tetrafluoroethylene that confers a unique combination of properties imparted from both fluorocarbon and hydrocarbon polymers. Moreover, undesirable chain scission reactions occurring during preirradiation grafting can be minimized by using ETFE, especially in combination with electron beam irradiation under inert atmosphere [63].

The base polymer film type and its properties (such as film thickness, extent of orientation, and molar mass) have significant effect on both the degree of grafting and resultant membrane properties [64, 65]. Walsby et al. [65] have reported that under identical conditions, grafting of styrene onto different base polymers yielded different graft levels. The authors indicated that graft levels were 5% for PTFE, 56% for PVDF, 28% for FEP, and 62% for ETFE. It

587 seems that the influence of the base polymer matrix on grafting is a complex 587
588 scenario. The differences obtained in graft level may be due to the different 588
589 radical concentrations, different structures of the radical centers, and differ- 589
590 ent degrees of crystallinity. Since the grafting essentially takes place in the 590
591 amorphous region, the high crystallinity of the polymer would provide lesser 591
592 radicals in the amorphous region accompanied by low monomer diffusion 592
593 for subsequent graft initiation and propagation. The glass transition tempera- 593
594 ture (T_g) may also contribute in terms of the mobility of the macromolecular 594
595 chains in the amorphous region. If the grafting is carried out at a tempera- 595
596 ture higher than the T_g , the enhanced mobility of chains would favor mutual 596
597 recombination of growing grafted chains, leading to the low graft levels [65]. 597
598 The radical concentration in PTFE tends to be two orders of magnitude lower 598
599 than in polyethylene and ETFE for an irradiation dose of 100 kGy and may 599
600 be one of the reasons for low graft levels [66]. ETFE films are found to yield 600
601 higher graft levels than that of FEP under identical grafting conditions. This 601
602 behavior may be attributed to the greater number of reactive sites available 602
603 for ETFE since more radicals are expected to be formed per kGy of radiation 603
604 dose (lower bond strength of C–H than C–C and C–F) [67, 68]. 604

605 Increasing the molecular weight of the base polymer film causes a decrease 605
606 in the DG. Melt flow index (MFI) measurements are especially useful for obtain- 606
607 ing both qualitative and quantitative information about the molecular 607
608 weight of polymers, chain scission, and crosslinking. It was reported that MFI 608
609 increases due to chain scission upon ETFE irradiation in air. Also, ETFE films 609
610 tend to undergo crosslinking during irradiation at room temperature under 610
611 inert atmosphere [64]. It is also observed that higher irradiation doses are 611
612 required for thinner base films than for thicker ones to achieve comparable 612
613 DG under identical grafting conditions. This may be attributed to the greater 613
614 extent of orientation of polymeric chains in the machine direction in thinner 614
615 films [63]. The extent of orientation has a significant effect on polymer 615
616 permeability, which decreases as the orientation increases [64]. A negative de- 616
617 pendence of grafting rate on film thickness for the grafting of acrylic acid 617
618 onto PTFE has been observed [69]. However, other investigations have shown 618
619 that the film thickness has no significant effect on grafting yield [70]. 619

620 Another interesting development in membrane fabrication has been the 620
621 use of porous base films [71]. The grafting of a monomer and subsequent 621
622 sulfonation still leads to porosity in the membrane bulk. However, this mem- 622
623 brane may be densified by impregnating it to substantially fill the porosity, 623
624 or the porosity may be collapsed by the application of pressure and heat. The 624
625 heating may be carried out to at least a melt flow temperature of the film but 625
626 at a lower melting temperature (T_m) than grafted side chains. 626

627 The pregraft storage of irradiated films is an important aspect of mem- 627
628 brane preparation. It has been observed that fluorinated polymers retain 628
629 their grafting ability for a longer period, irrespective of their chemical struc- 629
630 ture [47, 72]. Horsfall et al. [73] have shown that irradiated ETFE and PVDF 630

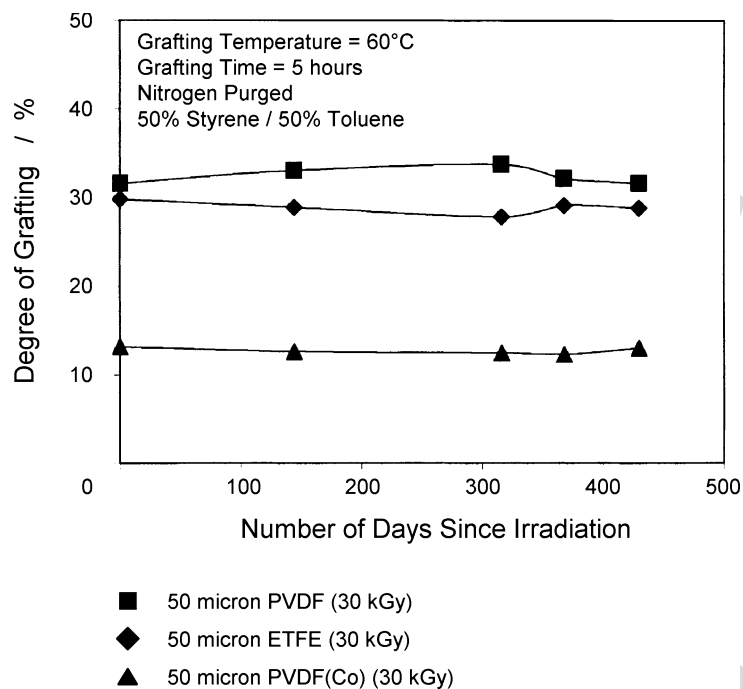


Fig. 3 Effect of low temperature storage on degree of grafting for the preirradiation grafting method [73]

films remain active even after more than a year of storage (Fig. 3). The storage of films may be accomplished at a low temperature of -18°C or even less. The behavior of polyethylene films has shown to be quite different as they undergo considerable loss in the DG with storage [52]. This opens up an interesting aspect in the preirradiation grafting of monomers onto fluorinated polymers, where irradiation may be carried out once and the resultant films may be stored for subsequent membrane fabrication. It was reported that the storage of irradiated FEP films at -60°C in the dark for 118 days had no significant effect on grafting [72].

2.4.2

Irradiation Dose and Dose Rate

The influence of the irradiation dose and dose rate on the grafting process has been the subject of detailed investigations. As the radiation dose increases, the number of radical sites generated in the grafting system also increases. This has been observed in the simultaneous radiation grafting of styrene into PTFE films, where the grafting increases almost linearly with the increase in the radiation dose and reasonably high graft levels up to 70% were

achieved [74, 75]. However, higher irradiation doses are not preferred due to the deterioration of mechanical properties [76].

Rager [77] has investigated the influence of irradiation dose on DG for grafting of styrene onto preirradiated FEP films (Fig. 4). Although DG increases as dose increases, it becomes more difficult to obtain higher degrees of grafting through a further increase in irradiation dose [77].

Chapiro [47, 48] demonstrated for the first time that the grafting yield increases with the total irradiation dose and is independent of the dose rate at low dose rates for simultaneous grafting of methyl methacrylate and styrene onto PTFE. It was emphasized that at low dose rates, the rate of polymerization was slow and grafting was diffusion controlled, whereas at high dose rates, the higher rate of polymerization exceeded the rate of diffusion and grafting was limited to the surface [47, 48]. As a matter of fact, the final DG increases with increasing dose and with decreasing dose rate for styrene grafting into PFA and PP [12]. It is important to note that a more efficient utilization of radicals is followed in simultaneous radiation grafting as compared to the preirradiation method. For the grafting of styrene onto Teflon-FEP films, a graft level of 40–50% is achieved using a radiation dose of 15 kGy in the simultaneous grafting method as compared to 100 kGy for similar graft levels in the preirradiation grafting method using gamma rays [72]. A significant fraction of radicals are deactivated during the course of preirradiation, and the polymer requires optimum activation by irradiation at additional doses to accomplish the high DG.

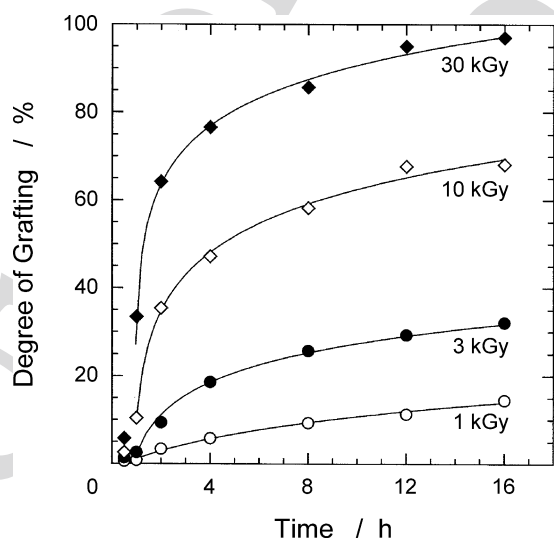


Fig. 4 Grafting kinetics as a function of preirradiation dose (grafting conditions: FEP 25 μm , 50% monomer concentration in isopropanol, 10% DVB, 60 $^{\circ}\text{C}$) [76]

It is observed that gamma and electron beam irradiation lead to identical degrees of grafting in FEP-g-polyacrylic acid systems [53]. However, the grafting of acrylic acid into polyethylene films shows much higher grafting under gamma irradiation than under electron beam irradiation [52]. The difference in the behavior of FEP and polyethylene films lies in the ability of the polyethylene film to hydroperoxidize under the influence of irradiation. Moreover, gamma irradiation is carried out for a longer period than electron beam irradiation. Therefore, the hydroperoxide build-up is much higher in gamma irradiated films and offers much higher graft levels than are achieved in electron beam. Certainly, the influence of crystallinity and other factors needs to be considered, which will be over and above the influence of the chemistry of the polymers. This is what has been observed in the preirradiation grafting of styrene onto PVDF, where the graft levels are two to four times higher than for poly(vinylidene fluoride-co-hexafluoropropylene) [65]. Looking at the composition of this copolymer, there is only 7% hexafluoropropylene present in the copolymer matrix, but it diminishes the grafting drastically. Hexafluoropropylene not only enhances the plasticization of the matrix but also interferes with the crystallization process and results in low crystallinity. As a result, the mobility of chains is enhanced and radical-radical crosslinking dominates over the grafting process.

The radiation dose rate has a profound influence on the equilibrium grafting of styrene onto various polymers, both in the vapor phase and in solution, using the simultaneous grafting method [75, 78, 79]. The initial rate of grafting in such systems increases with the increase in the radiation dose. This is the outcome of the efficient utilization of radicals in graft initiation and subsequent chain propagation. It needs to be mentioned here that in the initial stages, homopolymer formation is very limited and the grafting proceeds smoothly with time. Owing to the faster homopolymerization, the grafting at higher dose rates reaches saturation much faster than at lower dose rates. However, for a constant radiation dose, the higher dose rate results in low graft levels and, maybe because the radical concentration is so high, the radical-radical recombination becomes the dominant reaction [75, 78]. Under such conditions, radiolysis reaches equilibrium with radical deactivation and the radical concentration does not increase further with a further increase in the dose rate [31]. Moreover, the higher rate of homopolymerization follows at higher dose rate and leads to an increase in viscosity and a depletion in monomer content. As a result, the monomer availability through the grafted layers is reduced [79–81].

The order of dependence, determined as 0.64 for styrene grafting into FEP [72], 0.58 for grafting of acrylic acid into FEP [82], and 0.53 for styrene-acrylic acid [83], is in agreement with the theoretical value of 0.5 for free radical polymerization. Momose et al. [70] reported that for the grafting of α,β,β -trifluorostyrene (TFS) into ETFE, the grafting rate and final percent grafting increase with increasing preirradiation dose, with the dose exponent

of 0.3. The low dependence of grafting rate on the preirradiation dose may be attributed to the decay of trapped radicals due to the increased temperature during irradiation, radical decay during storage, or decay due to radical recombination. A similar trend has been reported for the radiation-induced grafting of acrylic acid onto PTFE [69, 84].

2.4.3 Monomer Concentration

Monomer concentration is the most dominant of the factors that significantly influence the grafting process. As long as the monomer accessibility to the propagating sites is facilitated, the grafting proceeds smoothly. This is the reason that an increase in the monomer concentration leads to an increase in the DG, which is observed for both the simultaneous and preirradiation grafting systems. The increase in grafting with increasing monomer concentration has been observed for the grafting of styrene and styrene–acrylic acid mixture into FEP films [55, 72]. Both the initial rate of grafting and equilibrium DG increase with the styrene concentration in the range of 20–100% [51]. This suggests that the grafting proceeds smoothly with the regular diffusion of monomer within the film. In contrast to the higher monomer dependence (1.9) observed for styrene grafting into FEP previously [72], a first-order dependence of the rate of grafting on the monomer concentration indicates that classical free radical polymerization kinetics operate in the system. However, the complexity arising from the extensive homopolymerization during the grafting may hinder monomer diffusion to the radical sites and may lead to diminishing grafting. This may lead to the maxima at specific monomer concentrations, beyond which the grafting would decrease rapidly. Liang et al. [85] have observed a maximum in the simultaneous radiation grafting of styrene into PTFE films, where the peak was observed at 70% monomer concentration in the grafting medium (Fig. 5).

Our group studied the influence of monomer concentration on styrene grafting into ETFE, using isopropanol/water as the solvent [80]. We found that the DG increases dramatically with an increase in the styrene concentration, until it reaches a maximum at 20% (v/v) styrene for reaction times above 2 h, and then decreases sharply as the concentration further increases. For grafting times below 2 h, this maximum is shifted to 50% (v/v) styrene. The increase in graft level was attributed to the increase in styrene diffusion and its concentration in the grafting layers. We determined the order dependence of the grafting rate on monomer concentration as 1.5. Nasef et al. [81] reported similar results for styrene grafting into ETFE in methanol as solvent. Moreover, these authors determined that the initial rate of grafting was significantly dependent on styrene concentration with an exponent as high as 2.0, which is not in agreement with a first-order dependence of free radical polymerization.

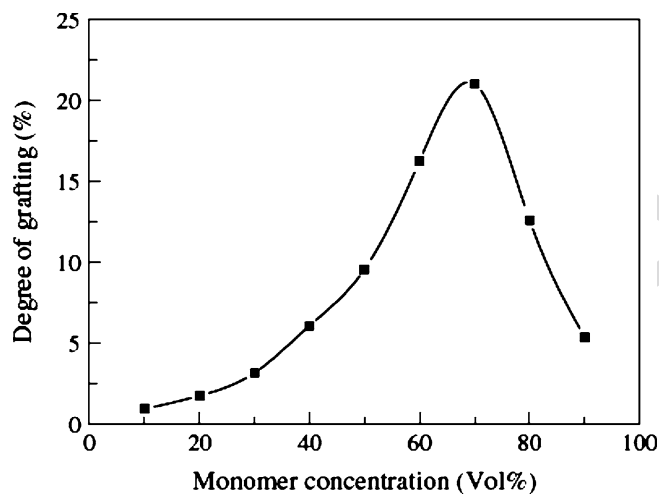


Fig. 5 Variation of DG with monomer concentration (grafting conditions: 20 kGy dose, 110 Gy min⁻¹ dose rate, dichloromethane as the solvent, 50 μ m film, ambient temperature, nitrogen atmosphere) [85]

It is important to see that a similar trend has been observed for the grafting of styrene into all three (PTFE, FEP, and PFA) films under identical conditions [75, 78, 86]. The DG increased dramatically with the increase in styrene concentration until it reached a maximum, and then decreased sharply as the concentration was increased further [74]. The authors emphasized that the DG of styrene in PTFE depends on both the number of radicals formed and the diffusion of styrene through the polymer matrix, and on its concentration in the grafting layers. Therefore, the increase in the DG in this system may be attributed to the increase in styrene diffusion and its concentration in the grafting layers. At very high concentrations of styrene, homopolymer formation was enhanced and the diffusion of styrene across the viscous medium was hindered. These studies are also supported by Cardona et al. [12] who observed that with increasing monomer concentration the DG reached a maximum and then decreased for styrene grafting into PFA and polypropylene.

The location of the maxima will be somewhat influenced by the nature of the solvent used in the reaction medium [56]. The initial rate of grafting should be largely dependent on the diffusibility of the monomer into the matrix and the grafting solvent must properly swell the grafted zone and make monomer diffusion possible. Such behavior has been proposed to be associated with styrene diffusion and its concentration within the grafted layers. It is stated that an increase in the monomer concentration up to 60% is accompanied by higher monomer availability within the bulk matrix, beyond which extensive homopolymerization leads to the depletion of monomer in

851 the grafting medium and subsequent reduction of styrene diffusion into the 851
852 film. The diffusion phenomenon has also been considered to be a decisive 852
853 factor in the grafting of styrene into ETFE [87]. The grafting of styrene with 853
854 acrylonitrile has been investigated recently [88]. It was observed that the 854
855 graft yield is considerably enhanced by the addition of acrylonitrile as the 855
856 comonomer. 856

857 Our patent search of last 5 years shows that although most of the stud- 857
858 ies have been directed to the use of styrene-based monomers [89–92]. Some 858
859 workers have tried to use substituted styrenes such as TFS to graft onto 859
860 FEP [93–95]. The DG in fact remained lower than that observed for styrene 860
861 grafting [93]. Momose et al. [96] has been granted a patent on the devel- 861
862 opment of TFS-based graft copolymer membranes using both low density 862
863 polyethylene and ETFE as the base polymers. Other patents describe graft- 863
864 ing of TFS and trifluorovinyl naphthalenes onto ETFE film, which facili- 864
865 tates the introduction of more than one sulfonic acid group per monomer 865
866 unit [97–102]. Considerably higher graft levels of $\sim 80\%$ and $\sim 44\%$ have 866
867 been achieved for TFS and *p*-methyl trifluorostyrene, respectively [100]. 867
868 A more recent patent describes the influence of the grafting mixture 868
869 alcohol/water on the grafting of TFS derivatives [103]. Furthermore, a novel 869
870 monomer combination, namely α -methylstyrene/methacrylonitrile, as graft- 870
871 ing component is discussed in [104]. 871
872

873 2.4.4

874 Grafting Temperature

875
876 The reaction temperature has a significant influence on the DG, irrespective 876
877 of the nature of the polymer and the monomer. The general observation has 877
878 been a decrease in the equilibrium DG as the reaction temperature increases. 878
879 On the other hand, the initial rate of grafting increases with increasing tem- 879
880 perature [72]. As a matter of fact, grafting is controlled by a cumulative effect 880
881 of the monomer diffusion within the polymer bulk, termination of the grow- 881
882 ing polymer chains, and the deactivation of the primary radicals. 882

883 As the reaction temperature increases, the monomer diffusivity within the 883
884 bulk also increases. This enhances the monomer accessibility to the graft- 884
885 ing sites within the polymer bulk. As a result, the rate of initiation and 885
886 propagation is enhanced. This is the reason that the initial rate of grafting 886
887 increases with the increasing temperature. The other aspect of grafting is 887
888 that the grafted zone remains swollen in the grafting medium, which leads 888
889 to high mobility of the growing chains within the matrix. Therefore, termi- 889
890 nation of the two growing chains by mutual combination becomes dominant 890
891 at higher temperatures. At the same time, the primary radical termination 891
892 may also accelerate by the time the monomer reaches their vicinity. In spite 892
893 of the higher rate of initial grafting, the final DG would decrease. A simi- 893
894 lar tendency has been reported for the grafting of styrene onto ETFE-based 894

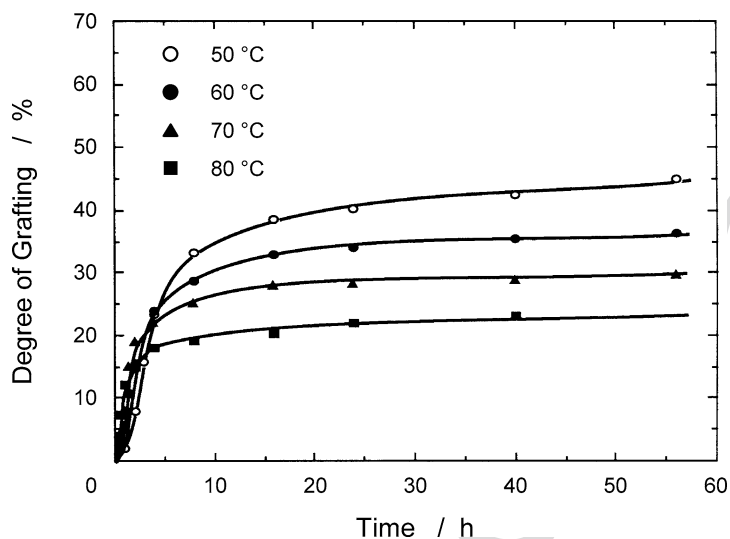


Fig. 6 Variation of DG with time at various temperatures (grafting conditions: 60 kGy dose, 60% monomer concentration, 50 μm film) [72]

films [64, 80, 81] and the grafting of TFS onto ETFE, FEP, PTFE, PFA, and LDPE films [105].

These observations are well in line with those of Rager [77]. The grafting studies were carried out at 50–85 °C and showed that the initial rate of grafting increases with the grafting temperature.

It may be mentioned that the T_g plays an important role in the grafting process. If T_g is lower than the grafting temperature, the mobility of chains is very high. Under such circumstances, the probability of primary radical termination becomes dominant. The final DG as a result may decrease. However, it may be overshadowed by the faster rate of chain initiation and higher monomer diffusivity at higher temperatures [72], as shown in Fig. 6. As a matter of fact, a sharp increase in the rate of grafting may be envisioned at the T_g of the specific polymer.

2.4.5 Grafting Medium

The graft copolymerization reaction is carried out by bringing the activated base polymer film into contact with the monomer in liquid or vapor form. The use of solvents in radiation grafting enhances the accessibility of monomer to the grafting sites due to the ability of the solvent to swell the base polymer. In poor swelling solvents, surface grafting occurs due to the slow down in monomer diffusion within the polymer. However, in good solvents,

939 bulk grafting is highly favored and homogenous grafting is obtained across 939
940 the film thickness. 940

941 The instantaneous swelling of the grafted matrix within the reaction 941
942 medium is an important factor that governs the grafting process. With the 942
943 progression of grafting, the polymer film is continuously being transformed 943
944 into a grafted structure. It is, therefore, the swelling of the grafted matrix in 944
945 the reaction medium of specific monomer composition that influences the 945
946 monomer diffusion within the film. The swelling at 10 and 60% monomer 946
947 concentration in the medium may be different than at higher concentrations 947
948 and may, therefore, be reflected in the low graft levels, as observed in Fig. 5. 948
949 This is further supported by the grafting of acrylic acid into polyethylene 949
950 films, where a similar maximum was observed at 25% monomer concentra- 950
951 tion [51]. It was observed that the swelling of the grafted film is considerably 951
952 reduced in a grafting medium containing monomer at higher than 25%, 952
953 which diminishes monomer diffusion and hence the availability to the prop- 953
954 agating chain within the bulk. 954

955 The nature of the solvent in the grafting medium is an interesting aspect 955
956 of achieving efficient graft polymerization. The type of solvent and the com- 956
957 position of the monomer/solvent mixture may influence the grafting kinetics, 957
958 the length of grafted chains, and polymer microstructure. Benzene, toluene, 958
959 dichloromethane, and alcohols (methanol, ethanol, and propanol) have been 959
960 employed as solvents for radiation grafting of styrene and styrene deriva- 960
961 tives. It seems that a combination of the polarity (solubility parameter) and 961
962 chain transfer constant of the solvent plays a major role in graft propaga- 962
963 tion. The use of dichloromethane has been observed to produce higher graft 963
964 levels over benzene and methanol [56]. The radical yield in different sol- 964
965 vent mediums has been established to be the reason behind such grafting 965
966 behavior. The radical yields of irradiated styrene solutions in methanol, cy- 966
967 clohexane, and benzene have the order methanol < cyclohexane < benzene. 967
968 The speculations of Nasef [78] and Dargaville et al. [13, 106] about the effect 968
969 of viscosity changes in the grafting medium (due to the insolubility of poly- 969
970 styrene in methanol as medium) on decreasing the graft levels do not seem 970
971 realistic. It may, in fact, be the lower swelling of the polystyrene-grafted ma- 971
972 trix in methanol/styrene mixture as the medium that lowers the monomer 972
973 diffusion within the film and results in a low DG. In such systems, the swelling 973
974 of the original polymer matrix is not as important as that of the grafted ma- 974
975 trix in the solvent medium [107]. This is achieved by using a solvent for the 975
976 grafted component in combination with the monomer. The propagating graft 976
977 chains become solvated in the surrounding medium. Since these chains are 977
978 part of the matrix, the whole matrix exerts swelling. As the grafting proceeds, 978
979 more polystyrene grafts are incorporated, leading to higher swelling of the 979
980 matrix, which allows more and more monomer to diffuse into the polymer 980
981 bulk for the propagation reaction. It is, therefore, the perfect matching of 981
982 the solubility parameter of the solvent with the grafted polymer domain that 982

would influence the swelling of the matrix during the grafting process. Benzene has a solubility parameter (18.6) much closer to that of styrene (19) as compared to dichloromethane (17.6) and methanol (29.7) [108]. The swelling of the polymer, therefore, would be higher in a solvent where the solubility parameters of the two are closer to each other. This would provide the least swelling in methanol but higher swelling of the grafted matrix in benzene medium for styrene-grafted films.

Cardona et al. [56] investigated the correlation of the efficiency of the grafting process with solubility parameters for polystyrene in various solvents. The authors reported that for grafting of styrene onto PFA in dichloromethane, the DG is higher than that of styrene in benzene and methanol. The chain transfer constants (0.15, 0.2, and 0.296 for dichloromethane, benzene, and methanol, respectively) were important parameters in this context. Low graft levels are obtained with solvents having a high chain transfer constant, since the growing chain will be quickly terminated, whereas solvents with low chain transfer constants enhance the propagation step and lead to higher grafting yields. The influence of solvent viscosity also plays an important role in surface graft-polymerization reactions [109].

An additional factor that originates from the use of a non-solvent medium, such as methanol, is the precipitation of the propagating chains and hindrance of diffusion of the monomer to the internal layers within the film, resulting in a decrease of the grafting [56]. However, recent investigations on the grafting of styrene onto PVDF and FEP films have exploited the use of alcohols as non-solvent for achieving higher graft levels [76,107]. The pre-irradiation grafting of styrene/divinyl benzene (DVB) onto FEP films is accelerated in alcohols in the order methanol < ethanol < propanol. A four-fold increase in grafting kinetics was observed when toluene was replaced by isopropanol and has been attributed to the Trommsdorff effect, which can occur in chain polymerization when the increasing viscosity limits the rate of termination because of diffusion limitations operating in the system [110].

This certainly opens up an interesting route for achieving membranes with reasonable DG for relatively lower irradiation doses, which might be beneficial in retaining the mechanical properties of membranes to a large extent. Walsby et al. [111] reported the grafting of styrene into PVDF in both propanol and toluene, where not only the grafting kinetics but also the structural properties of the grafted films were dependent on the type of solvent. Higher grafting rates and saturation DGs were obtained in a propanol-based system, which was unable to swell the polystyrene grafts. On the other hand, the grafting in toluene yielded more homogenous films with better surface aspects and mechanical properties. Reduced elongation at break and much rougher surface with large cavities were observed for the films grafted in propanol. The authors reported that the film was swollen very little by the grafting solution, and that propanol served as a diluent without any contri-

1027 bution to the swelling of the polystyrene grafts. The authors attributed the 1027
1028 higher grafting rate in propanol to the higher concentration of monomer in 1028
1029 the reaction zone, whereas the higher saturation DG was due to the higher 1029
1030 viscosity of the grafted zone, which prevents growing chain termination. 1030

1031 Some base polymers such as PTFE do not swell well in any common sol- 1031
1032 vent. For this reason, the grafting reaction is performed in aqueous medium. 1032
1033 Hegazy et al. [112] investigated the effect of various solvents on the radiation 1033
1034 grafting of methacrylic acid onto PTFE film. The authors demonstrated that 1034
1035 distilled water and methanol/water mixture (30/70 wt. %) are the most suit- 1035
1036 able solvents since the mixture swells the grafted regions. The increase in DG 1036
1037 upon addition of water to isopropanol was emphasized for styrene grafting 1037
1038 into FEP [76]. 1038

1039 The radiation grafting of TFS onto various fluorine-containing base poly- 1039
1040 mers, such as LDPE, ETFE, PFA, FEP, and PTFE has been accomplished by the 1040
1041 pre-irradiation method [105]. A proper examination of the swelling proper- 1041
1042 ties and solubility parameters of these polymer films in pure TFS showed that 1042
1043 LDPE yielded the highest, and PTFE led to the lowest graft levels. This is be- 1043
1044 cause of the fact that the sorption of liquid in polymer depends on the affinity 1044
1045 between the liquid and the polymer film. 1045
1046

1047 **2.4.6**

1048 **Additives**

1049
1050 The influence of additives such as acids to the grafting systems has been ex- 1050
1051 plored for achieving higher graft levels [78]. The addition of sulfuric acid has 1051
1052 been found to be effective in enhancing the DG of acrylic acid onto FEP and 1052
1053 polyethylene films [18, 21]. Styrene grafting onto polyethylene films has also 1053
1054 been observed to increase significantly in the presence of acids [113, 114]. 1054
1055 However, there are contradicting reports where no influence of organic and 1055
1056 inorganic acids was observed on the grafting of styrene into PTFE, PFA, and 1056
1057 FEP films [78]. Different hypotheses have been postulated for the enhance- 1057
1058 ment of the grafting but until today an exact mechanism of grafting in such 1058
1059 systems has not been proposed. 1059
1060

1061 **2.5**

1062 **Crosslinking**

1063
1064 Crosslinkers are used in conjunction with the monomer to achieve certain de- 1064
1065 sirable properties in the grafted membranes. The use of a crosslinker in the 1065
1066 grafting medium has been investigated by different workers to obtain mem- 1066
1067 branes that have improved stability in fuel cells [72, 115]. Lower graft levels 1067
1068 are achieved as the crosslinker content in the grafting medium increases. 1068
1069 This may be because the grafting starts at the film surface. In the presence 1069
1070 of crosslinker, the very first polystyrene-grafted chains become crosslinked. 1070

As a result, the mobility of chains is drastically lowered as compared to the crosslinker-free grafting reaction. Consequently, monomer diffusion to the grafting sites within the films is reduced. The higher the crosslinker content, the greater will be the crosslinking density of the grafted chains, which will hinder the monomer diffusion more and more, leading to comparatively low DG. However, it has been observed that crosslinkers may increase or decrease the grafting yield depending on their concentration [13]. At lower crosslinker concentration, the increased DG was attributed to enhanced branching reactions. At higher crosslinker concentration, on the other hand, a network structure was formed, which caused suppression in the swelling of the graft and an increase in viscosity of the grafting solution. This further resulted in a decrease of diffusion and in availability of the monomer and, consequently, the grafting yield was lower. These observations are well supported by the investigations of Rager [77] on styrene grafting onto FEP films. There was an initial rise in graft level for low a level of DVB content in the grafting medium and therefore the grafting decreased considerably. This has been attributed to the polyfunctional nature of the crosslinker.

The addition of crosslinking agents affects the kinetics of the grafting reaction. The addition of DVB decreased the initial rate of grafting and the limiting DG [116]. This is evident from the lower rates of grafting in crosslinked systems than in uncrosslinked ones. The rate of grafting for a crosslinker-free FEP-polystyrene system decreases from 3.6% per hour down to 2.2% and 1.4% per hour for 2 and 4% DVB content, respectively (Fig. 7). However, much higher values have been reported for the grafting of styrene/DVB onto PFA films using simultaneous radiation grafting, which may be attributed to the difference in the base matrix and the radiation dose rate. It was reported that the addition of DVB caused a significant decrease in the DG as a function of the DVB concentration for styrene grafting into PFA [115] and ETFE base films [117, 118].

The graft variation with the *N,N*, -methylene-bis-acrylamide as the crosslinker for grafting onto ETFE and FEP is quite different [119]. The grafting in fact did not show any specific trend with the increase in the crosslinker content.

The concept of double crosslinking has been examined previously by the use of DVB and triallylcyanurate (TAC) together for radiation grafting of styrene into FEP [72, 120, 121]. It was reported that TAC yielded improved mechanical properties and ionic conductivity [121]. Although it was found that TAC had a favorable promoting influence on the grafting kinetics, spectroscopic measurements failed to positively indicate that TAC was incorporated into grafted films and membranes [122]. Later, it was determined that TAC acted primarily as a graft-promoting additive rather than as a crosslinker [123].

The degree of crosslinking in the grafted film was found to be different from the composition of the grafting solution for FEP-based radiation grafted

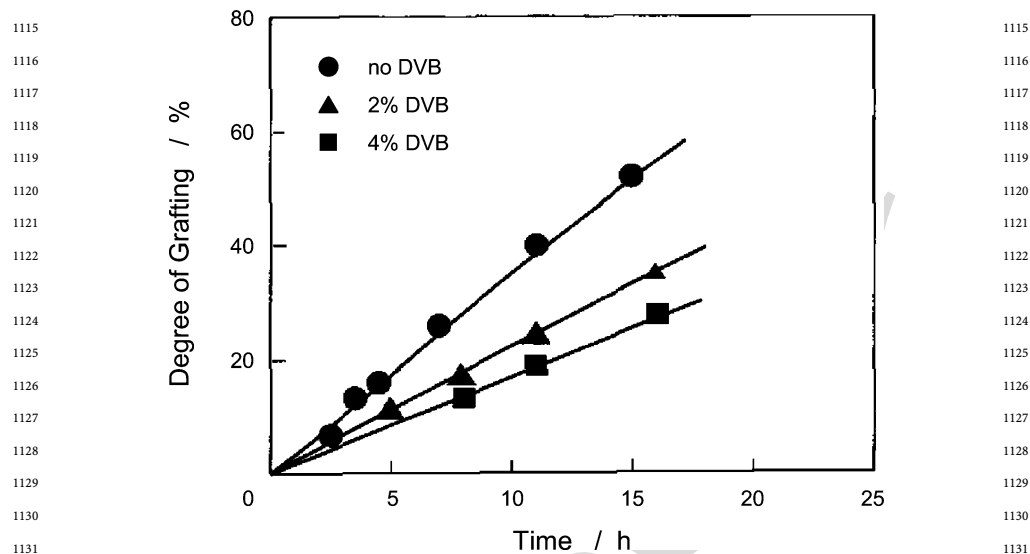


Fig. 7 Variation of DG with reaction time for different crosslinker contents [116]

films due to the different reactivity and diffusion coefficients of styrene and DVB in the film during the grafting process [124, 125]. It was observed that an increase in the degree of crosslinking decreases the membrane thickness, which means that crosslinking increases the structural density of the membranes. Moreover, the mobility of the protons in the membrane is reduced with increasing degree of crosslinking due to decreasing water uptake [125–127]. Moreover, Brack et al. [124] and Ben youcef et al. [118] reported that radiation grafted films are more highly crosslinked in their near-surface regions and thinner films are more extensively crosslinked.

Originating from the concept of crosslinking of fluoropolymers under irradiation at elevated temperature, grafting has been accomplished onto the crosslinked matrix so that the grafting-induced deterioration of mechanical properties may be compensated. As discussed in the preceding section, the crosslinking of PTFE is achieved in the molten state at a temperature of 340 °C. Surprisingly, the precrosslinked films (prepared under gamma irradiation doses of 60–320 kGy), lead to much higher polystyrene graft levels than the virgin one as given in Fig. 8 [128]. Such behavior is the result of two different factors operating in the system: (i) the availability of the amorphous area, and (ii) the radical site generation. It has been an established fact that grafting takes place predominantly within the amorphous region and on the crystal surfaces [127, 129]. The crystalline regions are impermeable structures and do not allow monomer diffusion and subsequent grafting with the radicals trapped within the crystallites [130]. Therefore, any process that leads to a decrease in the crystallinity would be expected to enhance the grafting

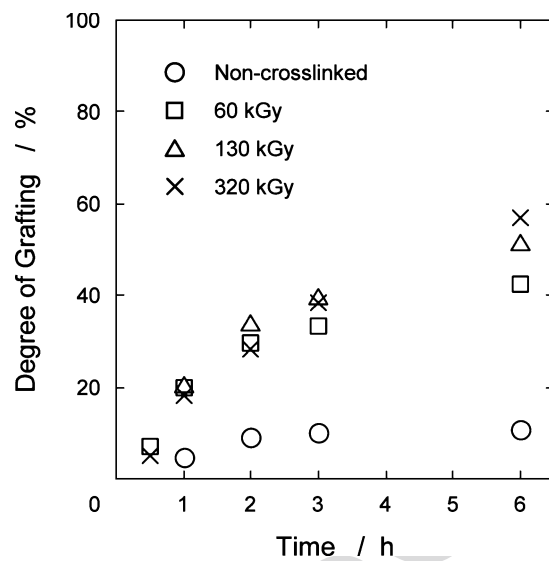


Fig. 8 Variation of DG with reaction time for styrene grafting into the PTFE films crosslinked with gamma rays at different doses (15 kGy preirradiation dose for the grafting reaction) [128]

reaction. The irradiation of PTFE is carried out in the molten state at a temperature of 340 °C where the crystallites are almost completely lost and the matrix behaves like the amorphous one. This state is achieved at irradiation at a high dose of 2 MGy, where the enthalpy of fusion in a differential scanning calorimetry reaches zero [131]. The irradiation at this stage would be favorable for the crosslinking reaction, providing a network structure due to the high mobility of chains. A crosslinked structure is more adapted to radical generation and has been found to have higher G values for the trapped free radicals than an uncrosslinked structure [32]. The radicals produced during the exposure of this crosslinked matrix would be more stable due to the reduced mobility of chains and would be available for graft initiation in contact with the monomer.

The precrosslinking of a polymer is an innovative approach to restoring mechanical strength. However, a proper monitoring of the precrosslinking dose has to be carried out to achieve reasonable graft levels. It is obvious that a precrosslinking dose that is too high may not bring about high graft levels [132]. It is observed that grafting enhances significantly with increasing dose but only up to a range of 50–500 kGy. Any further dose increase leads to loss in the grafting levels and very little grafting is obtained for film crosslinked at a dose of 2 MGy. This is because of the fact that the grafting ability of the polymer matrix is severely affected. The matrix is highly crosslinked to such an extent that the mobility of the molecular chains is suppressed. A crosslinked matrix may lead to lower diffusion of the monomer

1203 within the matrix and hence would have an adverse effect on graft propaga- 1203
1204 tion. However, it seems that the availability of the more amorphous region, 1204
1205 along with the higher availability of radical sites, overpowers the impact of 1205
1206 slow monomer diffusion. The temperature also has significant impact on the 1206
1207 grafting reaction. An increase in the temperature brings about lower graft 1207
1208 levels for films crosslinked at different doses. Here, the mobility of the grow- 1208
1209 ing chains at higher temperature increases to an extent that the bimolecular 1209
1210 termination of chains is facilitated. The termination of the primary radicals 1210
1211 would also be a dominant reaction and would contribute to the lower graft 1211
1212 levels. 1212

1213

1214 2.6

1215 Sulfonation

1216

1217 Sulfonation is the final step for the preparation of polystyrene-based mem- 1217
1218 branes for fuel cell applications. In this reaction a sulfonic acid group is 1218
1219 added to the aromatic ring by electrophilic substitution. Sulfonation can be 1219
1220 performed by several agents such as sulfuric acid, sulfur trioxide, sulfonyl 1220
1221 chloride, acetyl sulfate, and chlorosulfonic acid. 1221

1222 Sulfonation conditions have a significant effect on membrane properties 1222
1223 including ion exchange capacity, water uptake, and conductivity. Walsby 1223
1224 et al. [111] demonstrated that the reaction time, concentration of the sulfonat- 1224
1225 ing agent, and reaction temperature have a considerable effect on sulfonation 1225
1226 with chlorosulfonic acid. The authors reported that the sulfonation reaction 1226
1227 proceeds by a front mechanism, that the grafts at the surface are sulfonated 1227
1228 first, and that the rate of reaction depends on the diffusion of sulfonating 1228
1229 agent within the membrane. An increase in the concentration of the sulfonat- 1229
1230 ing agent and in reaction temperature facilitates the reaction; however, side 1230
1231 reactions, which cause a decrease in ion exchange capacity (IEC), water up- 1231
1232 take, and proton conductivity, are favored at these conditions. This indicates 1232
1233 that, although the use of harsher sulfonation conditions offers advantages 1233
1234 in terms of speed of the sulfonation process and oxidative stability, the IEC, 1234
1235 water uptake, and proton conductivity are decreased and the membrane be- 1235
1236 comes more brittle. Paronen et al. [6] emphasized that the rate of sulfonation 1236
1237 increased with short sulfonation time, because with longer sulfonation time 1237
1238 the hydrophilicity in the sulfonated regions governs the rate of sulfonation. 1238

1239 Sulfonation of FEP- and ETFE-based grafted films at PSI was performed by 1239
1240 using 30% chlorosulfonic acid in dichloromethane (at 95 °C, 5 h) and mem- 1240
1241 branes with reasonably good sulfonic acid content have been observed. Sul- 1241
1242 fonation conditions almost identical to those used at PSI have been used by 1242
1243 others for the sulfonation of PFA-*g*-polystyrene films, i.e., a mixture of chloro- 1243
1244 sulfonic acid and 1,1,2,2-tetrachloroethane (30 : 70 v/v, 90 °C, 5 h) [133]. 1244
1245 Phadnis et al. [83] performed the sulfonation of styrene-acrylic acid grafted 1245
1246 FEP films in concentrated sulfuric acid (at room temperature). Concentrated 1246

1247 sulfuric acid and refluxing under nitrogen (at 95 °C) has been used for PVDF-
1248 *g*-polystyrene films [134]. The attempts to sulfonate PVDF-*g*-polystyrene 1248
1249 films in concentrated sulfuric acid at temperatures between 21 and 95 °C 1249
1250 and in acetyl sulfate/dichloroethane solutions at 50 °C yielded low degrees of 1250
1251 sulfonation, and the sulfonation was mainly restricted to the surface [111]. 1251
1252 This may be due to the insufficient reactivity of these sulfonating agents. 1252
1253 In addition, sulfuric acid may not be able to penetrate into the hydrophobic 1253
1254 matrix. 1254

1255 The number of sulfonic acid groups in the membrane increases with the 1255
1256 increase in the DG. At higher styrene concentrations more benzene rings 1256
1257 are in contact with sulfonic acid groups, which results in more sulfonic acid 1257
1258 groups in the membrane. However, the efficiency of the sulfonation reaction 1258
1259 depends to large extent on whether or not the membrane is grafted through 1259
1260 its thickness [111]. If the samples contained a core of ungrafted parts, sul- 1260
1261 fonation was incomplete at room temperature due to insufficient swelling of 1261
1262 the samples and the difficulty of diffusion of the sulfonating agent. It was 1262
1263 observed that full sulfonation of surface grafted samples can be achieved at 1263
1264 higher temperatures. 1264

1265 3 1265

1266 **Characterization and Structure of Grafted Films and Membranes** 1266

1267 The characterization of membranes is essential for correlating their perform- 1267
1268 ance in fuel cells. It is the interface of the membrane that interacts with 1268
1269 the electrode and hence a proper surface morphology may in fact improve 1269
1270 the performance of the membrane electrode assembly. Membrane prepar- 1270
1271 ation involves the graft polymerization of a monomer, usually styrene, and 1271
1272 subsequent sulfonation of the grafted matrix. This transforms a hydropho- 1272
1273 bic fluorinated structure into a hydrophilic ion exchange matrix. Therefore, 1273
1274 the polymer film undergoes drastic modification in terms of the physico- 1274
1275 chemical properties and morphological nature, depending on the irradiation, 1275
1276 grafting, and sulfonation conditions. 1276
1277 1277
1278 1278
1279 1279
1280 1280

1281 **3.1** 1281

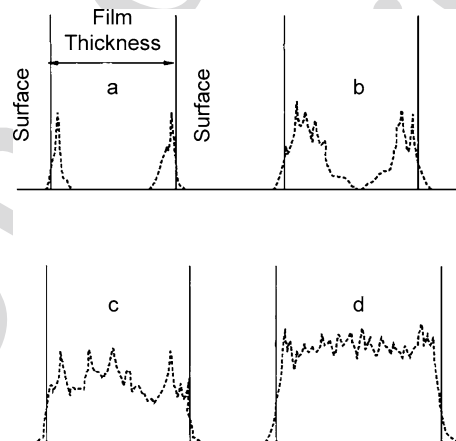
1282 **Graft Mapping** 1282

1283 The most important requirement of the membrane is the homogeneous dis- 1283
1284 tribution of grafts across the membrane matrix. X-ray microprobe analysis 1284
1285 (XMA) has been an effective way to monitor the graft distribution within the 1285
1286 membrane matrix. The X-ray fluorescence for sulfur may be monitored across 1286
1287 the membrane thickness and provides useful information about the distri- 1287
1288 bution of the sulfonic acid groups and, hence, of the grafts across the ma- 1288
1289 trix [127, 135, 136]. It was observed that the grafted phase was initially con- 1289
1290 1290

1291 centrated at the film surface. The low graft levels of $\sim 3\%$ film shows a very 1291
 1292 high concentration of sulfur only on the surface, as presented in Fig. 9 [127]. 1292
 1293 The presence of sulfur in the middle of the membrane may be seen with 1293
 1294 a further increase in the DG. The two zones from both sides approach each 1294
 1295 other towards the middle and subsequently a homogeneous distribution of 1295
 1296 sulfur, or in other words polystyrene grafts, is achieved. This indicates that 1296
 1297 the grafting is a time-dependent process and that the homogeneous structure 1297
 1298 is possible only at a specific graft level and beyond a specified grafting time, 1298
 1299 irrespective of the grafting method used to produce the membranes. For instance, 1299
 1300 a homogenous distribution of grafts was achieved at DG higher than 1300
 1301 20% for FEP-based films [87, 116]. 1301

1302 This further substantiated the idea that grafting proceeds through a grafting 1302
 1303 front mechanism and that DG above 30–35% is required for two grafting 1303
 1304 fronts to meet and form a network for proton conduction [137]. It is also observed 1304
 1305 that an inhomogeneity, in the form of bubbles on the membrane surface, 1305
 1306 is created after sulfonation of grafted films with graft levels below 11%. 1306
 1307 The membrane inhomogeneity arises due to the presence of hydrophilic sulfonated 1307
 1308 polystyrene chains in the surface layer of the hydrophobic perfluorinated 1308
 1309 FEP matrix [138]. 1309

1310 It was observed that the addition of crosslinker (2–4% DVB) to styrene 1310
 1311 considerably affected the homogeneity profile behavior [116]. The distribution 1311
 1312 became practically homogenous across the whole width of the film 1312
 1313 and the homogeneity increased at 4% DVB [116, 139]. That behavior was attributed 1313
 1314 to the decreased rate of diffusion in the grafted zone near the surface, 1314
 1315 an increase in the rate of termination of growing chains, and a decrease in the 1315
 1316 concentration of styrene in surface layers [116]. The observations for the TFS- 1316
 1317 1317



1333 **Fig. 9** Distribution of sulfur as determined by microprobe measurements in the transverse 1333
 1334 plane of FEP-based membranes with different DG: **a** 3.1%, **b** 5.9%, **c** 13.6%, **d** 27% [127] 1334

1335 grafted systems have been found to be completely different. It was observed 1335
1336 that for TFS grafted onto PTFE and ETFE, although the graft chain distribu- 1336
1337 tion is almost constant over the range of film thickness for ETFE-based films, 1337
1338 the grafted PTFE exhibited two peaks (XMA profile) located $\sim 10 \mu\text{m}$ inside 1338
1339 the film surface. That was attributed to a better monomer diffusivity in an 1339
1340 ETFE base film than in a PTFE base film [105]. 1340

1341 Micro-Raman mapping is another interesting tool for analyzing the depth 1341
1342 profile of the grafted component within the membrane matrix [12, 57, 79]. 1342
1343 The ratio of the intensity of the Raman peaks associated with the aromatic 1343
1344 band in polystyrene at 1601 cm^{-1} and in the fluorinated matrix, such as 1344
1345 PFA at 996 cm^{-1} at the surface and along the cross-section, provides infor- 1345
1346 mation about the distribution of the grafts. The graft penetration tends to 1346
1347 be higher at higher radiation doses. Likewise, the vapor phase grafting has 1347
1348 been observed to remain confined to the surface layers only [57, 79]. Hietala 1348
1349 et al. [140] observed that for polystyrene-grafted PVDF films, although poly- 1349
1350 styrene distribution was homogenous on the surface at high graft levels, the 1350
1351 surface became quite heterogeneous at low graft levels. 1351

1352 Hegazy et al. investigated the cross-sections of the poly(acrylic acid)- 1352
1353 grafted FEP films [141] and PTFE films [142] by X-ray microscopy. It was 1353
1354 observed that the monomer was limited to the surface at low graft levels. 1354
1355 However, it penetrates the entire film and homogenous grafting throughout 1355
1356 the entire film is observed for high graft levels. 1356

1357 It has been reported that the geometric dimensions of the styrene-grafted 1357
1358 FEP films vary linearly, but not equally, with the increase in the DG. For in- 1358
1359 stance, for a graft level of 52%, an increase of 25% in length as well as width 1359
1360 and 45% increase in thickness have been obtained. Equal distribution of poly- 1360
1361 styrene within the FEP matrix prepared via simultaneous radiation grafting, 1361
1362 at least for a graft level of 21%, has been monitored by Fourier transform 1362
1363 infrared spectroscopy (FTIR) and attenuated total reflection spectroscopy 1363
1364 (ATR) [126]. Similarly, FTIR-ATR was used to determine the surface grafting 1364
1365 yields for styrene grafted onto ETFE by measuring the ratio of absorbance 1365
1366 of the polystyrene peak at 699 cm^{-1} (C–C wagging band) to the ETFE matrix 1366
1367 band at 1046 cm^{-1} ($-\text{CF}_2$ stretching vibration) [143]. 1367

1368 Confocal Raman microscopy has been employed for the investigation of 1368
1369 the changes in membrane composition after fuel cell experiments for PVDF- 1369
1370 based radiation grafted membranes. In fact, severe degradation due to loss of 1370
1371 polystyrene sulfonic acid (PSSA) was observed during the fuel cell run and 1371
1372 only 5–10% of the initial content was found to be left behind. It has been 1372
1373 reported that the degradation is an inhomogenous process that is different 1373
1374 over the membrane surface and through the membrane depth [144]. It was 1374
1375 proposed that the deterioration of fuel cell performance was because of the 1375
1376 loss of entire PSSA chain segments rather than desulfonation [145] and is 1376
1377 supported by the studies on ETFE-based membranes [146] and FEP-based 1377
1378 membranes [125]. 1378

3.2

Surface Chemistry and Surface Morphology

The surface and wetting properties are known to influence the adhesive and bonding properties of materials [147]. The contact angle measurements of membranes provide useful information on the surface and interfacial behavior. Graft management within the membrane may take place in such a way that the surface is rendered hydrophobic in spite of the hydrophilic nature of the grafted component [148]. This could happen either during the grafting process or during the post-grafting treatments of the copolymer matrix. A fundamental investigation of the wetting and surface energy properties of commercial perfluorinated membranes and uncrosslinked radiation grafted membranes indicated that the surface properties of uncrosslinked radiation grafted membranes are similar to those of commercial perfluorinated membranes having similar ion-exchange capacities [148]. In addition, the contact angle of both the grafted and the sulfonated ETFE membranes shows distinct variations with different wetting agent [149]. The polystyrene-grafted films do not show any appreciable change with water as a function of graft level, but measurements with methylene iodide as a probing liquid indicate a decrease in the contact angle with an increase in graft level. At higher graft levels, the contact angle has been observed to behave identically to that for a pure polystyrene surface. This indicates that the surface of the membrane is rich in polystyrene. Sulfonation changes the wetting behavior drastically; the contact angle of water is significantly reduced to 32° for a graft level of 82%. This is an indication of the surface rendered hydrophilic due to the presence of sulfonic acid groups. However, absolute values of the contact angle have been observed to vary significantly in different investigations [85]. Maybe, the nature of the base matrix and the sulfonation process have some impact on the wetting behavior. The maximum degree of sulfonation in PTFE graft copolymer membranes has been reported to be 50% and may account for the higher contact angle in these membranes as compared to ETFE membranes [149].

Contact angle measurements on the fully swollen form of the radiation grafted membranes using several polar, non-polar, hydrogen-bonded, and non-hydrogen-bonded liquids have been performed by Brack et al. [149]. The high contact angle of water on the FEP-based membrane revealed the hydrophobic nature of the membrane due to the crosslinking and relatively low degrees of grafting. Moreover, crosslinking has a tendency to limit the mobility of chain segments. Due to restricted mobility it was difficult to undergo surface reconstruction to adjust the most favorable local structure at a surface or interface. The membrane cannot adapt a hydrophilic surface when it is exposed to water during an earlier swelling process [150].

X-ray photoelectron spectroscopy (XPS), provides quantitative information on surface chemical structure, chemical composition, and chemical bonding, and is one of the most extensively used methods for radiation

1423 grafted films and membranes. This method is useful for investigating the 1423
1424 surface chemistry taking place during the grafting and sulfonation pro- 1424
1425 cesses [151]. XPS has the ability to probe the surface within a few nanometers 1425
1426 and, therefore, interesting information about the chemical composition at 1426
1427 a few top layers is obtained. As a result, the polystyrene graft within and 1427
1428 on the surface of the fluorinated matrix may be monitored [151]. The evolu- 1428
1429 tion of the C–F and the C–H : C–F ratio with respect to the DG or irradiation 1429
1430 dose, as is evident from Fig. 10, indicates a high concentration of C–H, i.e., 1430
1431 polystyrene chains on the surface [56]. Consequently, a significant loss of 1431
1432 the fluorinated species in the PFA matrix is observed. A strong increase in 1432
1433 the relative amount of C–H bonds at a dose of about 50 kGy is the indica- 1433
1434 tion of grafting taking place at the surface right from the beginning of the 1434
1435 irradiation. As the radiation dose increases, more grafting takes place on the 1435
1436 surface and in the bulk and, finally, the plateau beyond a dose of 250 kGy sug- 1436
1437 gests that at least the top few nanometers of the surface can be considered to 1437
1438 be the polystyrene grafts. Moreover, the matrix with lower crystallinity has 1438
1439 a higher C–H : C–F ratio, suggesting more polystyrene grafts on the film. This, 1439
1440 in principle, substantiates the earlier assumption that the lower crystallinity 1440
1441 makes the matrix more amenable to monomer diffusion and subsequent 1441
1442 grafting with the radical sites. 1442

1443 It was observed that the surface composition is strictly governed by the 1443
1444 degree of crosslinking in FEP membranes [139]. The uncrosslinked FEP-g- 1444
1445 polystyrene copolymer films show a well-defined C–H signal at ~ 286 eV, 1445
1446 confirming the presence of polystyrene grafts on the surface. The absence of 1446
1447 the –C–F signal in the uncrosslinked films is an indication of the abundance 1447
1448 of the polystyrene on the surface. However, this signal is slowly lost in films 1448
1449 prepared under increasing crosslinker content, while the C–F signal increases 1449
1450 indicating that the polystyrene grafts are more and more confined to the bulk 1450
1451 of the matrix. In addition, the sulfonated matrix shows a similar but weaker 1451
1452 trend. The C–F signal was visible for the uncrosslinked membrane. 1452

1453 Nasef et al. [151, 152] investigated the structural changes enhanced by 1453
1454 styrene grafting and subsequent sulfonation of PTFE film as well as a vari- 1454
1455 ation of the DG of PTFE-based membranes. It was reported that the mem- 1455
1456 branes had side-chain grafts of polystyrene and structures composed of car- 1456
1457 bon, fluorine, sulfur, and oxygen. The authors determined that the base film 1457
1458 undergoes structural changes in terms of chemical composition and shifting 1458
1459 in binding energy. Although the binding energies of C1s, F1s, S2p, and O1s 1459
1460 were found to be independent of DG, the amount of each component was 1460
1461 shown to be dependent on DG. 1461

1462 It was observed that polystyrene grafted in a PVDF matrix under irradi- 1462
1463 ation with γ -rays or heavy ion irradiation exhibited very large domains, when 1463
1464 investigated using small angle X-ray and neutron scattering (respectively, 1464
1465 SAXS and SANS) [153, 154]. The characteristic length of the ionic domains 1465
1466 is observed at very low angles because of the large size of the domains. The 1466

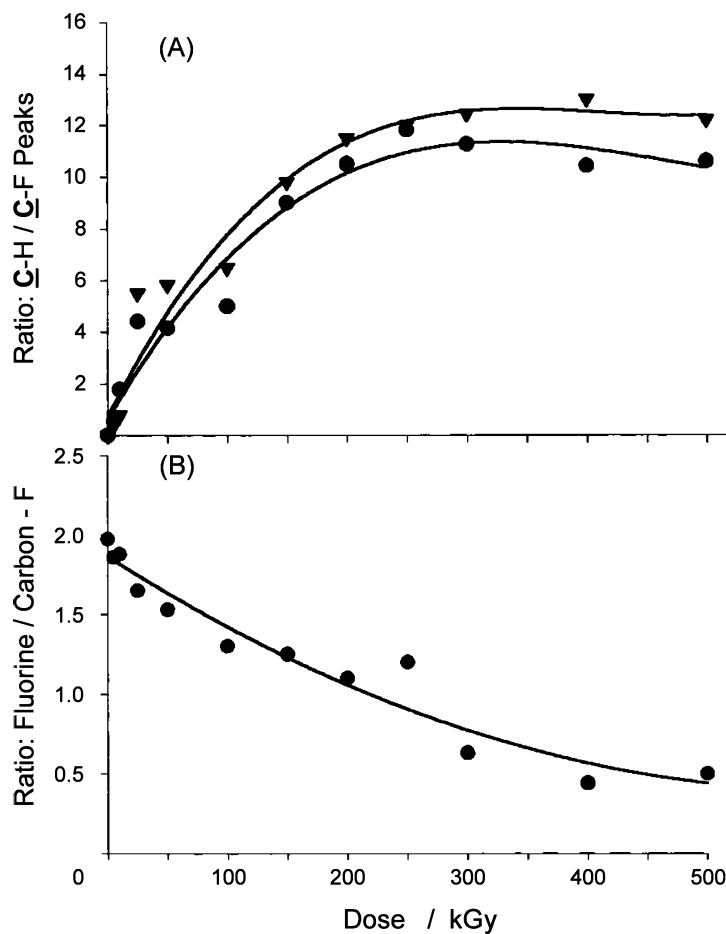


Fig. 10 Plots of **a** the atomic ratio of hydrogenated carbons (C-H) to fluorinated carbons (C-F) and **b** the ratio of fluorine (F1s) to fluorinated carbons (C-F) as a function of applied grafting dose: PFA-A (\blacktriangledown) and PFA-B (\bullet). The irradiation was undertaken in nitrogen gas, with 50% styrene solutions in dichloromethane, and 6.5 kGy h^{-1} dose rate) [56]

broad maximum at large angles is only observable in membranes swollen in heavy water. The grafting in irradiated PVDF gives rise to a swelling on a microscopic scale, which is limited to low grafting levels ($< 10\%$). The small-angle upturn observed for a water-swollen sulfonated sample was similar to that observed for the same sample before sulfonation, due to a dilution of the sulfonated groups by water swelling. Structural investigation of radiation grafted membranes by SAXS in the dry state of the membrane show a strong upturn in intensity, as observed over the investigated angular range. In the swollen state, a very broad maximum with low intensity was deter-

1511 mined [155–157]. This difference was attributed to a characteristic distance 1511
1512 between ionic domains. 1512

1513 Recently, the influence of crosslinking with DVB on the morphology of 1513
1514 polystyrene-grafted FEP films was probed by SANS and a characteristic in- 1514
1515 fluence was observed. These results corroborate the interpretation of results 1515
1516 obtained by DSC and TGA, namely the picture of a morphology for a two- 1516
1517 phase semi-crystalline polymer, with the grafting component essentially be- 1517
1518 ing present in the amorphous phase (Mortensen et al. unpublished results). 1518

1519 Surface morphology is one the most important aspects of membrane 1519
1520 design. The morphology is strongly influenced by the nature of the graft 1520
1521 medium, which takes into account both the monomers and the diluents or ad- 1521
1522 ditives. Scanning electron microscopy (SEM) has been an effective tool for vi- 1522
1523 sualizing the surface texture [158]. A distinct difference becomes visible in the 1523
1524 styrene-grafted PVDF vis-à-vis the hexafluoropropylene copolymer of PVDF 1524
1525 membranes. The PVDF membrane shows a much larger but wrinkled struc- 1525
1526 ture on the surface in comparison to the hexafluoropropylene-based PVDF 1526
1527 membrane, which tends to be smoother. These results exhibit the importance 1527
1528 of styrene diffusion within the films, as the monomer diffusion is faster in 1528
1529 the latter film and the polystyrene-grafted layer formation becomes less pro- 1529
1530 nounced, leading to the smoother surface. It should be mentioned here that 1530
1531 the composition of the grafting medium has a strong influence over the sur- 1531
1532 face morphology. The grafting of styrene onto PVDF introduces roughness, 1532
1533 as is evident from SEM characterization [107]. The grafting in toluene as 1533
1534 medium leads to some inhomogenous surface. However, isopropanol as the 1534
1535 grafting medium introduces cavities of $\sim 10 \mu\text{m}$ diameter. This is essentially 1535
1536 due to precipitation of the polystyrene chains in isopropanol, which leads to 1536
1537 phase separation within the grafted matrix and as a consequence, is reflected 1537
1538 as cavity formation. It is important to mention here that a change in the opac- 1538
1539 ity of the grafted films is observed in the presence of the crosslinker. These 1539
1540 films turn light transparent at higher crosslinker concentration [77]. Cross- 1540
1541 sections of the membranes may be visualized under SEM, where micrographs 1541
1542 can be seen with distinct variation in the morphology of the membrane. 1542
1543 A dark region in the middle and a clean region at one edge become evident 1543
1544 for the ungrafted and grafted regions, respectively [152]. 1544

1545 Atomic force microscopy is another interesting tool for investigating the 1545
1546 surface morphology. A three-dimensional profile of the grafted structures 1546
1547 may be achieved, which offers a more informative evaluation than SEM. The 1547
1548 investigations on the surfaces of polystyrene-grafted PVDF films and mem- 1548
1549 branes have revealed the heterogeneous character of membrane surfaces with 1549
1550 alternation of PVDF and PSSA [140]. It was reported that after grafting the 1550
1551 surfaces were found to be inhomogenous, and that blobs of polystyrene (do- 1551
1552 main size of $0.1\text{--}2 \mu\text{m}$) were observed on the surface. Such a behavior arises 1552
1553 due to the incompatibility of the grafted component and the base polymer 1553
1554 films. As a matter of fact, the grafted components remain as distinct isolated 1554

1555 phases within the fluorinated matrix and remain visible as inhomogeneity
1556 on the film surface. However, after sulfonation the blobs disappeared and the
1557 membrane surface became visually smoother [140]. Similarly, it was reported
1558 previously for polystyrene-grafted FEP membranes that the incompatibility
1559 between the hydrophobic perfluorinated backbone and the hydrophilic PSSA
1560 was overcome at high degrees of grafting and that the whole matrix behaved
1561 as a hydrophilic matrix. As a consequence, the film swells homogeneously in
1562 water leading to a smooth surface [138].
1563

1564 3.3

1565 Thermal Characterization

1566
1567 Thermal behavior of radiation grafted films and membranes have been investigated
1568 mainly by using thermogravimetric analysis (TGA) and differential
1569 scanning calorimetry (DSC). It has been observed from TGA that a two-step
1570 degradation pattern is exhibited by styrene-grafted FEP-based films, indicating
1571 that the degradation of grafted polystyrene and that of the FEP base
1572 polymer occurred independently from each other [114, 159, 160]. In addition,
1573 the degradation pattern was found not to be much affected by the
1574 DG [101]. This shows that the polystyrene-grafted FEP copolymer films behave
1575 as a distinct two-phase system, where the polystyrene moiety forms
1576 a separate micro-domain within the FEP matrix. Similar observations have
1577 been made for the polystyrene-grafted FEP, ETFE, and PVDF films [161, 162],
1578 PFA films [115, 163], and PVDF films [164].

1579 Sulfonation changes the stability pattern of membranes completely. The
1580 thermal degradation behavior of FEP-based membranes has been investigated
1581 previously by TGA in combination with FTIR and mass spectroscopy [160].
1582 As presented in Fig. 11, unlike the two-step degradation pattern of the grafted
1583 films, a three-step weight loss pattern was observed for radiation grafted membranes
1584 and has been ascribed to dehydration of the membrane, desulfonation,
1585 and de-aromatization reactions, and finally degradation of the backbone [160].
1586 a similar degradation pattern has been reported in the literature for the other
1587 radiation grafted membranes [135, 159, 161, 162, 164, 165].

1588 It is important to understand that every step of membrane preparation,
1589 i.e., irradiation, grafting and sulfonation leads to certain changes in the crystalline
1590 structure. For instance, the incorporation of polystyrene grafts caused
1591 an increase in amorphous fraction and restricted the mobility of the chains,
1592 and T_g increased. Similarly, the incorporation of the sulfonic acid groups
1593 caused ionic interactions, and the mobility of the molecular chains and T_g
1594 increased. The slight decrease in T_m was attributed to the changes in original
1595 crystal size by styrene grafting and little disruption in the crystalline
1596 region was observed [165]. Moreover, the grafting process leads to a decrease
1597 in the heat of fusion with an increase in the DG in FEP-g-polystyrene copolymer
1598 films [114]. This arises because of the dilution effect on inherent crys-

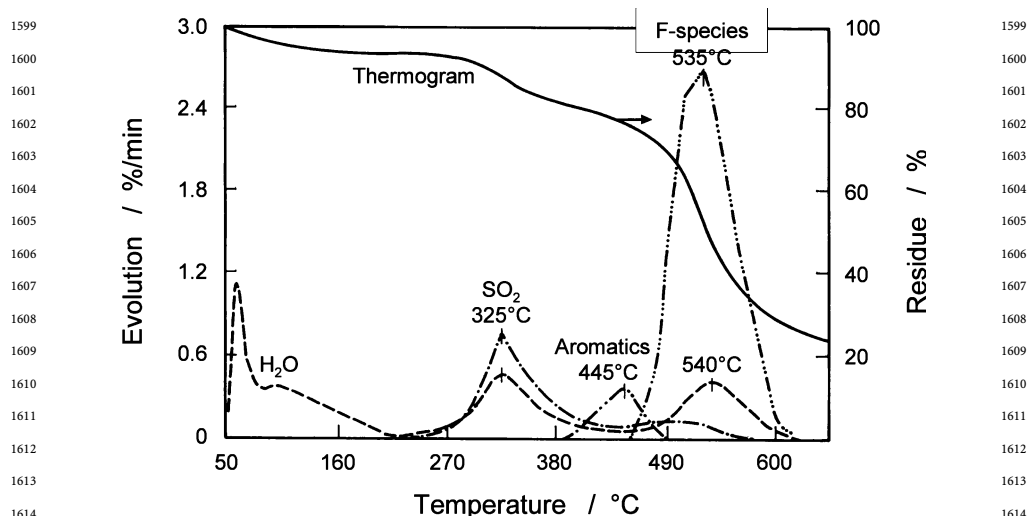


Fig. 11 Gaseous evolution pattern of FEP-based membranes [160]

tallinity of FEP by the incorporation of amorphous polystyrene grafts within the non-crystalline region of the film. According to the investigation of Cardona et al. [163] for PFA-based films, a relatively small decrease in inherent crystallinity after grafting has been observed since grafting occurred preferentially in the amorphous phase of the semi-crystalline polymer (diffusion was slow and radicals were less reactive in the crystalline phase). However, sulfonation of the grafted films leads to further decrease in the heat of fusion of the membranes (Fig. 12), and consequently decreases crystallinity [166]. It has been indicated that the loss of crystallinity in membranes is in addition to the changes induced by the dilution effect. These changes have been identified as crystal defects, as is evident from the loss of heat of fusion in Fig. 12. It is in fact the hydrophilic PSSA domains within the hydrophobic FEP matrix that absorb water and so strong hydrophilic-hydrophobic stresses develop in the water-swollen membrane and may be the reason for the distortion of the crystallite. This sounds reasonable considering the distortion of crystallites that has been observed in the sulfonation of polyethylene [167] and recently also in PVDF-g-PS [169].

The trend in the crystallinity of PTFE-based membranes seems to be different than for FEP membranes [151]. The grafting of styrene into PTFE film decreases the crystallinity from 43.2 to 32.1% for a graft level of 36%, which subsequently reduces to 21% on sulfonation. Although this trend accounts for the preservation of the inherent crystallites during the grafting and sulfonation processes, the authors attribute it solely to the dilution effect [169]. It seems that crystal distortion is also prevalent in this system because the crystallinity decreases more (21%) than if only the dilution effect persisted

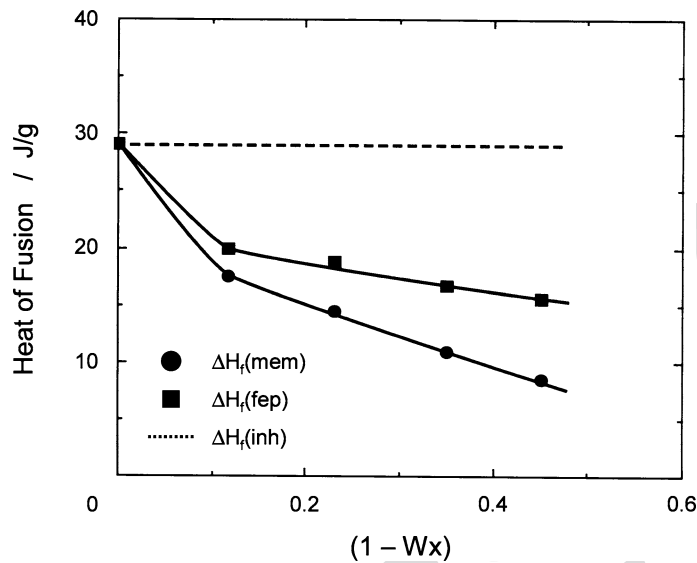


Fig. 12 Variation of the heat of fusion of the membrane $\Delta H_{f(mem)}$, FEP component in the membrane $\Delta H_{f(fep)}$, and inherent value $\Delta H_{f(inh)}$ with the cumulative weight fraction of acid group and water ($1 - W_x$) [166]

(23.4%). However, there have been more investigations on the crystallinity variations of grafted films and sulfonated membranes based on poly(vinyl fluoride), PVDF, ETFE, and FEP using DSC [65]. It was observed that the dilution effect of grafted component is the only factor that influences the overall crystallinity, suggesting that the inherent crystallinity remains intact. This is supported by a decrease in crystallinity content with the increasing graft level of styrene-grafted PFA films, which is interpreted as indicating that this behavior is the dilution and partial destruction of the inherent crystallinity [115].

In a recent investigation, the influence of the irradiation and grafting processes on the crystallinity have been investigated for three base polymers by DSC [161]. The grafting process has been found to have the largest effect on base polymer crystallinity and resulted in a reduction of crystallinity in all cases. In addition, the authors reported as a result of TGA investigation that the extent of fluorination of the base polymer, the graft level, and the irradiation method all had important influences on the thermal degradation of the films and the activation energy for this process. These results were nicely confirmed for ETFE-*g*-polystyrene-based membranes [118, 162].

The X-ray diffraction studies have been interesting in supporting the observations on the crystallinity of membranes determined by DSC. The crystalline reflections in graft copolymer membranes with different degrees of grafting fall on identical angles. However, their intensity decreases, suggest-

ing a decrease in their inherent crystallinity [74, 169]. A detailed characterization of a number of radiation grafted fluorinated films has been carried out to give a deeper glimpse of the crystal structure and orientation of the crystalline zone [170]. The grafting and subsequent sulfonation of the films led to a decrease in the crystallinity in each step again, because of the incorporation of amorphous polystyrene chains in the non-crystalline region of the film. The full width at half-maximum did not change, indicating the stability in the orientation. This shows that the grafted chains are bound to the amorphous region and do not disturb the crystalline region of PVDF films.

The effect of crosslinking on the degradation of the FEP-based grafted films and membranes have been investigated using TGA coupled to FTIR [171]. It was found that crosslinking causes a shift of the de-aromatization reaction to higher temperatures; however, the desulfonation reaction was shifted to lower temperatures. DVB increases the thermal stability of polystyrene grafts, facilitates the desulfonation process, and leads to a higher ash content.

3.4

Mechanical Properties

Mechanical integrity is one of the most important prerequisites for fuel cell membranes in terms of handling and fabrication of membrane electrode assemblies, and to offer a durable material. Robust fuel cell membranes are required because of the presence of mechanical and swelling stresses in the application [172]. Moreover, membranes should possess some degree of elasticity or elongation to prevent crack formation.

Typical mechanical properties of polystyrene-grafted FEP- and ETFE-based membranes have been investigated previously [62, 63, 146]. It has been reported that ETFE-based grafted films and membranes exhibit comparably better mechanical properties than FEP-based ones since ETFE films are available at higher molecular weight, which enhances breaking strength and flexibility. In addition, FEP undergoes a greater extent of chain scission reactions compared to ETFE. For both ETFE and FEP, the membranes from electron beam irradiation under inert atmosphere have better mechanical properties than the membranes from gamma irradiation under air. It is observed that thinner membranes possess poorer mechanical properties than the thicker membranes. Crosslinker also affects the mechanical properties and highly crosslinked membranes have poorer mechanical properties than the membranes with lower levels of crosslinker [62, 63]. The mechanical properties of FEP-based membranes are superior to those of the grafted films and may be due to the plastizing effect of water in the swollen membrane [62]. Similarly, the tensile properties of the grafted films and membranes are also reported [65].

The influence of irradiation dose and grafting solution on the mechanical properties of styrene-grafted FEP-based films has been investigated previ-

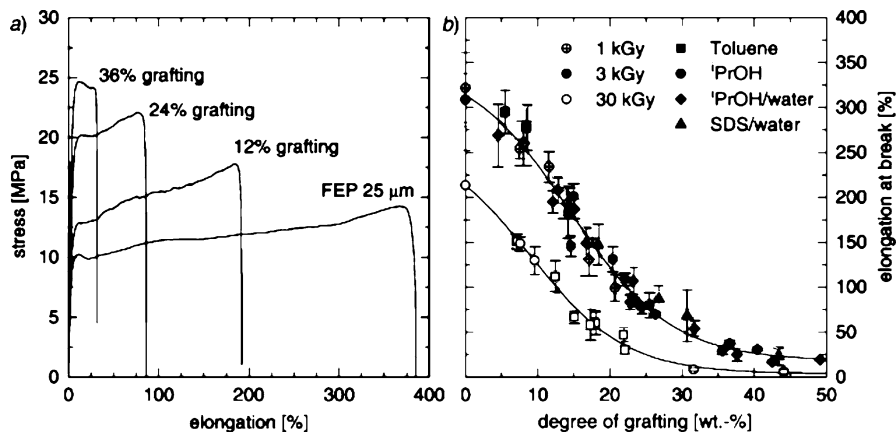


Fig. 13 a Stress–strain curves for pristine FEP and grafted films with different DG. b Elongation at break of grafted films as a function of DG, preirradiation dose, and type of solvent: FEP 25 μm, 10% DVB in solvents toluene, isopropanol (*i*PrOH), isopropanol/water mixture (*i*PrOH/water), and sodiumdodecyl sulfate/water (SDS/water) [76]

ously [76]. The elongation values of grafted films are lower than those of the unmodified base polymer (Fig. 13a). As presented in Fig. 13b, an increase of irradiation dose leads to considerable deterioration in the mechanical properties of pristine FEP and grafted FEP films. The loss in elongation at break with higher irradiation dose is attributed to an increased radiation damage to the trunk polymer. However, the type of solvent used during grafting has no significant effect on the elongation at break (Fig. 13b). Walsby et al. [107] has pointed out that the mechanical properties of PVDF-*g*-polystyrene films are seriously affected by the nature of the grafting medium. It was shown that better mechanical properties were obtained for the films in toluene compared to those in isopropanol. These and other authors have also reported that the mechanical properties of the base film in the machine direction and transverse direction differ significantly [118]. Although the film elongates several times compared to its initial length in the machine direction, elongation is negligible in the transverse direction.

4 Fuel Cell Application

4.1 Membrane Properties Relevant to Fuel Cell Application

In the polymer electrolyte fuel cell (PEFC), proton-conducting cation-exchange membranes are used as electrolyte, which consist of an organic

polymer structure (crosslinked or uncrosslinked) containing pendant acid functional groups, e.g., sulfonic acid $-\text{SO}_3\text{H}$ [173]. Hydration of the membrane (i.e., incorporation of water molecules into the polymer structure) leads to dissociation of the acid groups into mobile $\text{H}^+(\text{aq})$ and immobile anions fixed to the polymer backbone. The resulting nanophase-separated structure is an interpenetrating network of hydrophobic polymer backbone material providing structural integrity and aqueous domains allowing proton transport within water-containing channels. The proton conductivity of the material depends on the density of acidic groups, their dissociation constant ($\text{p}K_a$), and on the mobility of the proton, which is governed by the level of hydration (i.e., the water content of the membrane) and the geometry (dimensions, connectivity) of the hydrophilic channels.

4.1.1 Ion Exchange Capacity

The requirement of water within the polymer structure as a proton transport medium limits the operating temperature of such membranes to below 100°C at moderate pressure. Alternative membrane concepts using anhydrous proton conduction are under development. Among the approaches, phosphoric acid-doped polybenzimidazole appears among the most promising. Here, protons are transported via a phosphoric acid network [174]. The technology of radiation grafting has not been adopted for the preparation of water-free membranes for high temperature operation, with the exception of the work mentioned in a patent by Toyota [175]. The method involves grafting of vinylpyridine onto an ETFE or PVDF backbone, followed by imbibition of the film with phosphoric acid. However, due to the limited references in this area, the following discussion will be concerned with radiation grafted membranes with a water-based proton transport mechanism.

In radiation grafted proton-exchange membranes, the structural integrity of the component originates from the base polymer film, and the proton conduction functionality is introduced with the graft component. Therefore, it can be expected that the proton conductivity will be a function of the number of exchange sites within a given membrane portion. The corresponding parameter is the ion exchange capacity (IEC), which is defined as:

$$\text{IEC} = \frac{n(\text{SO}_3\text{H})}{m_{\text{polymer}}}, \quad (1)$$

where $n(\text{SO}_3\text{H})$ is the number of exchange sites and m_{polymer} is the dry mass of the polymer. The IEC is determined by titration [149]. Obviously, the IEC increases as a function of DG (Fig. 14). For styrene-grafted membranes, the

theoretical IEC, assuming one sulfonic acid group per aromatic ring, is:

$$IEC_{th} = \frac{DG}{M_S + DG \cdot M_{SSA}}, \quad (2)$$

where $M_S = 104 \text{ g mol}^{-1}$ is the molar mass of styrene, and $M_{SSA} = 184 \text{ g mol}^{-1}$ is the molar mass of styrene sulfonic acid. It can be deduced from Eq. 2 that for high levels of grafting, the theoretical IEC approaches the value for pure sulfonated polystyrene, which is:

$$\lim_{DG \rightarrow \infty} IEC_{th} = \frac{1}{M_{SSA}} = 5.4 \text{ mmol g}^{-1}. \quad (3)$$

Yet, the IEC value gives no indication about the distribution of the exchange sites across the membrane thickness, which is of course of paramount importance for the protons to be transported all the way from anode to cathode. It is possible that the conductivity of a membrane sample is low, even if the IEC is at acceptable levels. This happens when the grafting has not proceeded through the entire thickness of the base polymer film. Often, a threshold DG is observed, below which the conductivity is unmeasurably low, and above which acceptable conductivity is obtained [157, 176, 177]. The explanation is that at low degrees of grafting, the center of the membrane remains un-

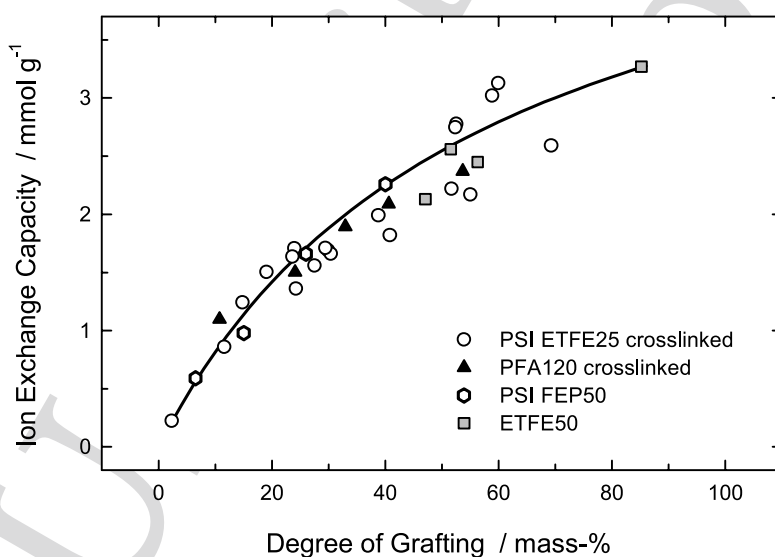


Fig. 14 The ion exchange capacity (IEC) of styrene-grafted and sulfonated membranes as a function of DG. The *solid line* represents the theoretical IEC for 100% degree of sulfonation, corresponding to one sulfonic acid group per aromatic ring (data for PFA120 crosslinked redrawn from [130]; data for ETFE50 redrawn from [213]; data for PSI FEP50 redrawn from [151])

grafted, and only above the threshold do continuous hydrophilic channels for proton transport exists through the membrane.

4.1.2 Water Uptake

As the acidic groups need to dissociate for the proton to become mobile, one can expect that the water content of the membrane will also have a strong influence on conductivity. Proton transport occurs either via hopping of protons from one water molecule to the next (Grotthus mechanism) or via the net transport of H_3O^+ or other aggregates of water and H^+ [178]. Evidently, as the DG increases and with it the number of ion exchange sites, so will the hydrophilicity of the material, resulting in an increase of the water uptake. The water uptake (ϕ) is expressed according to:

$$\phi = \frac{m_w - m_d}{m_d} 100\% , \quad (4)$$

where m_w and m_d are the mass of the wet and dry membrane, respectively. A quantity that is often used to describe the water uptake of an ion exchange membrane is the so-called hydration number (λ), which is the number of

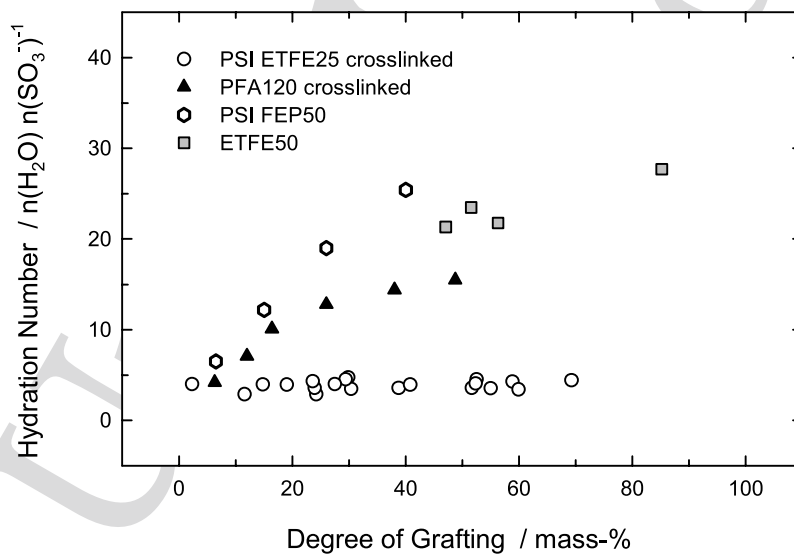


Fig. 15 Water uptake, expressed as the number of water molecules $n(\text{H}_2\text{O})$ per sulfonic acid site $n(\text{SO}_3^-)$, as a function of DG (data for PFA120 crosslinked redrawn from [200]; data for ETFE50 redrawn from [213]; data for PSI FEP50 redrawn from [135])

water molecules $n(\text{H}_2\text{O})$ per sulfonic acid site $n(\text{SO}_3\text{H})$. λ is defined by:

$$\lambda = \frac{n(\text{H}_2\text{O})}{n(\text{SO}_3\text{H})} = \frac{m_{\text{water}}}{\text{IEC} \cdot M_{\text{water}}}, \quad (5)$$

where $M_{\text{water}} = 18 \text{ g mol}^{-1}$ is the molar mass of water. It is usually observed that the hydration number increases with the DG (Fig. 15), which points to the fact that as the membrane gets more hydrophilic upon incorporation of the graft component, the acidic sites become increasingly hydrated.

Monomers that act as crosslinking agents, such as DVB or bis(vinyl phenyl)ethane are introduced as comonomers, in some cases to improve the dimensional and chemical stability of the membrane (as shown in Sect. 2.5). It is observed that the IEC of crosslinked membranes does not differ from that of uncrosslinked membranes with the same graft level (Fig. 14) [115, 118, 121, 125, 157]. This means that the introduced ionic sites are equally accessible through the hydrophilic domains in crosslinked membranes, regardless of the more constrained polymer framework, at least up to the level of crosslinking agent investigated, which is around 20%. The amount of swelling is substantially reduced upon crosslinking, which is the reason for the improved dimensional stability of crosslinked membranes (Fig. 15) [115, 125, 127]. Consequently, the hydration number decreases as the degree of crosslinking increases at a given graft level. We will see in the next section how this affects the conductivity of the material.

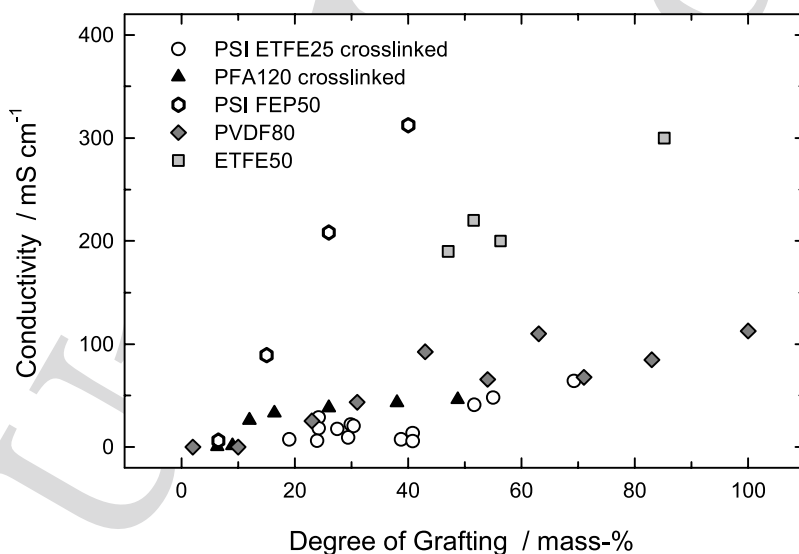


Fig. 16 Conductivity of various radiation grafted membranes as a function of DG at room temperature (data for PFA120 crosslinked redrawn from [200]; data for ETFE50 redrawn from [213]; data for PSI FEP50 redrawn from [135]; data for PVDF80 redrawn from [187])

4.1.3

Conductivity

As expected, the conductivity of radiation grafted ion exchange membranes increases with increasing DG, both for crosslinked and uncrosslinked membranes. There is, however, a tremendous range of conductivity values reported by different authors. The values range from < 1 up to 300 mS cm^{-1} at room temperature in fully hydrated (i.e., liquid–water equilibrated) state. The measured conductivity is governed or influenced by a number of parameters, above all by the distribution of the graft component across the membrane, as mentioned [157, 176, 177]. The base film thickness also appears to have an influence in some cases, thicker base films yielding a higher conductivity [63, 125, 146]. It is conceivable that this is a surface effect, i.e., that regions close to the surface of the irradiated film are less grafted, potentially due to loss of radical sites caused by exposure of the material to oxygen and water in the air. On the other hand, this thickness effect can also be observed for Nafion [146], so it may also be a physical effect, presumably unfavorable aggregation or conformation of the ionophoric side chains close to the surface.

Proton conductivity (σ_{H^+}) can be related to the proton diffusion coefficient D_{H^+} using the Nernst–Einstein equation [179]:

$$\sigma_{\text{H}^+} = \frac{D_{\text{H}^+} c_{\text{H}^+} z^2 F^2}{RT}, \quad (6)$$

where c_{H^+} is the volumetric density of protons and z , F , R , and T have the usual meaning. Proton diffusion in water and proton-exchange membranes is thermally activated, hence the quantity $\sigma \cdot T$ shows a temperature dependence of Arrhenius type. For perfluorosulfonic acid membranes such as Nafion, activation energies between 12 and 15 kJ mol^{-1} are obtained [180]. As a comparison, 10.3 kJ mol^{-1} are found for pure water [181]. For radiation grafted membranes, only limited data is available. For the conductivity of uncrosslinked PVDF-based membranes in the temperature range between 20 and $70 \text{ }^\circ\text{C}$, an activation energy similar to Nafion 105 was found, yet quantitative values were not given [182]. Changes in membrane morphology and water uptake with temperature were put forward as further contributions to the increase in conductivity, in addition to the higher mobility of the protons. The resistance of membranes from Solvay, based on ETFE and crosslinked with DVB, was measured in situ during DMFC operation in a temperature range between 90 and $130 \text{ }^\circ\text{C}$ [183], and an activation energy of around 18 kJ mol^{-1} was calculated. A study carried out in the authors' laboratory, using water-swollen crosslinked and uncrosslinked FEP- and ETFE-based membranes with 20 – 25% graft level, showed higher activation energy for the crosslinked membranes (15.0 – 15.5 kJ mol^{-1}) compared to the uncrosslinked ones (14.0 – 14.5 kJ mol^{-1}), which may be a consequence of higher association

of the protons with the counterions or polymer in crosslinked membranes, which have lower water uptake [184].

In addition to the conductivity in the water-swollen state, the conductivity of the fuel cell membrane under non-saturated water vapor conditions is of importance as, during cell operation, partial drying of the membrane and electrodes may occur. Also, fuel cell operation with partially humidified or even dry reactant gases is highly desirable to minimize system complexity. Walsby et al. [185] has investigated the influence of relative humidity on conductivity of radiation grafted membranes (Fig. 17). It was found that although the radiation grafted membranes displayed a superior conductivity at a relative humidity of 100%, the value dropped below that of Nafion at relative humidities between 40 and 85%. Below 40%, all the membranes exhibited poor conductivity of around 1 mS cm^{-1} or lower. The different behavior could again be indicative of a dissimilar microstructure, polymer domain morphology, or extent of hydrophilic-hydrophobic phase separation [178]. There is no literature data on the polymer morphology of radiation grafted membranes; it is, however, likely that the microstructure will depend to a large extent on base film type, graft level, extent of crosslinking, and other design and process parameters. A sorption curve qualitatively similar to the data shown in Fig. 17 for radiation grafted membranes is observed for sulfonated poly(ether ketone) membranes. The strong drop in conductivity below 90% relative humidity is attributed to a less effective phase separation in polymer

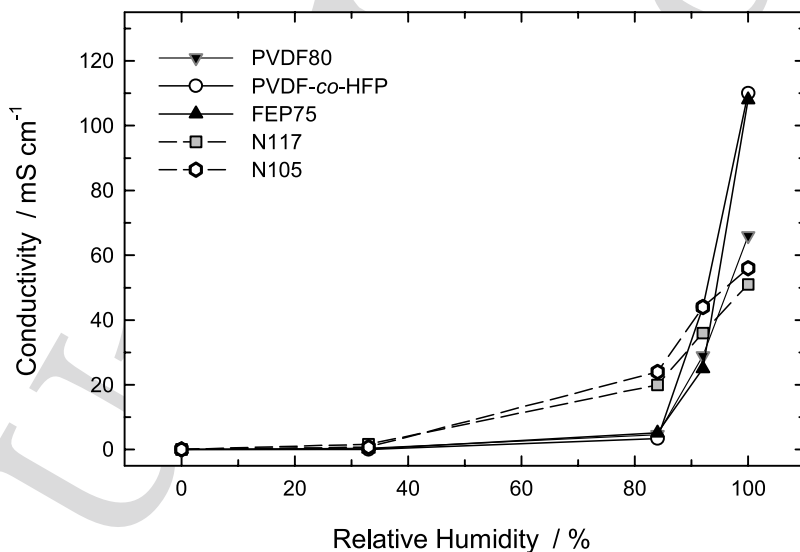


Fig. 17 Influence of relative humidity on conductivity at room temperature. Radiation grafted membranes are not crosslinked and have DG between 34 and 40% (redrawn from [206])

Table 4 Physical properties of radiation grafted membranes with different extent of crosslinking (redrawn from [121])

Base polymer	Degree of grafting (mass %)	Degree of crosslinking ^a (mol %)	Ion exchange capacity (mmol g ⁻¹)	Water content ^b (H ₂ O/SO ₃ H)	Conductivity ^c (mS cm ⁻¹)
FEP-50	19.1	0	1.39	27.2	98
FEP-50	18.8	3	1.07	25.9	93
FEP-50	19.6	6	n/a	11.9	63
FEP-50	19.0	12	1.27	7.0	28

^a Determined in grafted films via FTIR^b Swollen in boiling water^c Determined in situ, fuel cell temperature of 40 °C, using equipment built in-house

backbone and proton conducting aqueous channels, a less favorable percolation of the hydrophilic domains, and higher localization of the protons due to the higher pK_a value compared to Nafion [186].

For crosslinked membranes, the situation is somewhat different. Depending on the extent of crosslinking, excessive water uptake under fully humidified conditions is inhibited due to the network of covalent bonds in the polymer [184]. The effect of crosslinking on water uptake and conductivity has been investigated by Büchi et al. [125], as given in Table 4. For membranes of similar DG, it is observed that an increase in crosslinker content results in a decrease of water uptake and conductivity [118]. If the conductivity is plotted versus the water content, an approximately linear correlation is found, suggesting that the proton mobility is governed to a large extent by the hydration level of the material.

4.2

Performance in Fuel Cells

In PEFC, the membrane, together with the electrodes, forms the basic electrochemical unit, the membrane electrode assembly (MEA). Whereas the first and foremost function of the electrolyte membrane is the transport of protons from anode to cathode, the electrodes host the electrochemical reactions within the catalyst layer and provide electronic conductivity on the one hand, and pathways for reactant supply to and removal of products from the catalyst on the other hand. The components of the MEA need to be chemically stable for several thousands of hours in the fuel cell under the prevailing operating and transient conditions. PEFC electrodes are wet-proofed fibrous carbon sheet materials of a few 100 μm thickness. The functionality of the proton-exchange membrane extends to requirements of mechanical stability to ensure effective separation of anode and cathode, also under aggravated

2083 conditions such as operation on reactant gases below the water vapor saturation
2084 point, fuel cell start-up, and transient load. For a detailed review of fuel
2085 cell performance and in situ characteristics of radiation grafted membranes,
2086 the reader is referred to an article from the authors' laboratory published
2087 recently [43]. In this contribution, the insights are presented in a distilled
2088 manner with condensed facts and conclusions.

2089 **4.2.1**

2090 **MEA Fabrication**

2092
2093 The formation of an intimate contact between membrane and electrodes
2094 during MEA fabrication is of high importance to minimize interfacial volt-
2095 age losses. When using radiation grafted membranes together with elec-
2096 trodes containing Nafion as ionomer, it has been found that the membrane-
2097 electrode interface is of inferior quality compared to when Nafion is used
2098 as membrane, resulting in a higher resistance and/or insufficient adhesion
2099 or delamination [61, 182, 187]. The likely reason for this is the mismatch in
2100 ionomer type between the membrane and electrode catalyst layer. Huslage
2101 et al. [60] and Gubler et al. [61] found that dip-coating FEP-based radia-
2102 tion grafted membranes in solubilized Nafion prior to hotpressing leads to
2103 an improved fuel cell performance and lower impedance of the single cell.
2104 Furthermore, these authors showed that hotpressing with the membrane in
2105 wet state resulted in an improved membrane-electrode interface compared to
2106 when hotpressing with the membrane in dry state, which can be explained on
2107 the basis of the water acting as a plasticizer, allowing polymer flow during the
2108 hotpressing process.

2109 **4.2.2**

2110 **Fuel Cell Testing**

2111
2112 Generally, little fuel cell testing using radiation grafted membranes has been
2113 reported in the literature, compared to the total number of articles on the
2114 subject. Frequently, characterization is restricted to the membrane, and is
2115 not extended to include fabrication of MEAs and fuel cell testing. Important
2116 insights relating to electrochemical performance, membrane-electrode inter-
2117 face properties, membrane integrity, and lifetime are therefore missing. Of
2118 the studies published that include fuel cell test results, selected articles are
2119 reviewed in the following sections to highlight specific aspects.

2120 **4.2.3**

2121 **Water States and Water Management**

2122
2123 In the characterization of fuel cell membranes, there are a number of import-
2124 ant materials and component properties that have to be assessed in order to
2125
2126

determine the applicability and operability in the fuel cell environment Fig. 18. Since proton mobility within the polymer structure is a strong function of the water content, the water uptake and transport properties of the membrane are of paramount importance, determining the water profile through the thickness of the membrane as well as in-plane. Water transport mechanisms in the polymer are diffusion due to a gradient in water content, hydraulic permeation as a consequence of a pressure gradient between anode and cathode, and electroosmotic drag, i.e., water flux coupled to proton transport.

The states of water have an important role to play in determining the transport behavior of protons in membranes. The water directly associated with ionic sites in a membrane may behave in a way different from normal water due to its strong association in the form of hydrogen bonding or polar interactions with the functional sites within the membrane. Such water does not show any phase transition such as crystallization or melting in the temperature range 200–273 K. Using DSC, three different types of water molecules have been identified in sulfonated FEP-*g*-polystyrene membranes, which may be categorized as the freezing free, freezing bound, and non-freezing water [188]. The relative ratio of these three types of water molecules depends on the DG. The non-freezing water per ionic sites remains independent of the DG. However, the freezing free and freezing bound water per ionic site tends to increase with the DG (Fig. 19). The non-freezing water was evaluated to be six to eight water molecules per ionic site in membranes with DG in the range 15–40%. Recent investigations on membranes based on styrene grafting on different films showed that the non-freezing water remains almost the same, irrespective of the chemical nature of the membranes, and corresponds to ten water molecules per ionic site [185]. This is further supported by the studies on crosslinked PVDF membranes.

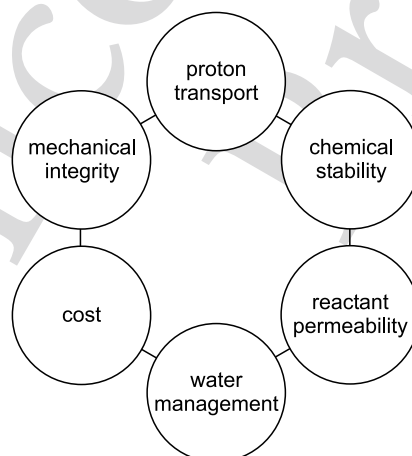


Fig. 18 Requirements for fuel cell membranes

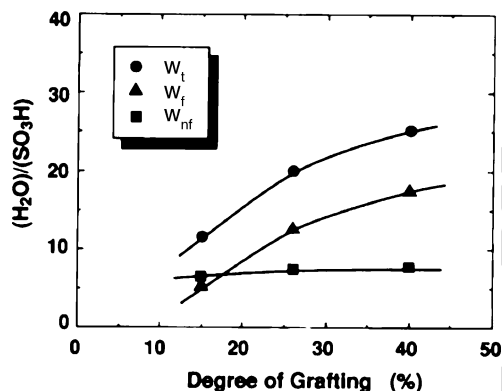


Fig. 19 Variation of water/ionic site ratio with DG for FEP-based membranes: W_t total water uptake, W_f freezing uptake, and W_{nf} non-freezing water uptake [188]

It may be stated that any increase in the water content with higher graft levels is associated with the incorporation of freezing water and should facilitate the ionic mobility [188]. With the increase in each grafting molecule, the hydrophilicity of the membrane matrix increases and crystallinity decreases. The structure as a result becomes more amenable to water penetration within the matrix. The crosslinking, however, influences the water uptake and its states. Highly crosslinked membranes developed from the DVB–styrene system do not show any freezing water and all of the water that accounts for the swelling of the membrane tends to be non-freezing in nature [129].

4.2.4

Reactant Permeability

Whereas uniform distribution of water within the membrane is desired, the permeability of the material to reactants (i.e., hydrogen or methanol and oxygen) has to be low to prevent direct chemical reaction between fuel and oxidant, which may lead to hotspots and, eventually, pinhole formation. Methanol permeability is a major challenge in the direct methanol fuel cell (DMFC), largely because methanol transport is strongly correlated with water transport, leading to significant penalties in fuel efficiency and poor cathode performance [189].

4.2.5

Chemical Stability

Chemical integrity of the polymer has to be maintained at the desired operating conditions for the designated operating time. The hostile fuel cell environment is a consequence of the simultaneous presence of H_2 , O_2 , H_2O_2

as intermediate, the noble metal catalyst, and possibly metallic contaminants such as Fe ions. It is widely accepted that radicals generated within this environment, such as hydroxyl ($\text{HO}\cdot$) and hydroperoxyl ($\text{HO}_2\cdot$) radicals, chemically attack the polymer, causing chain scission [190–195].

4.2.6 Mechanical Integrity

Furthermore, the material has to exhibit sufficient mechanical stability in order to fulfil its separator function. Not only tensile strength and elongation at break values have to be considered, but also dimensional stability upon swelling, and resistance to crack formation and propagation. Creep of the polymer is likely to occur because the water-swollen membrane is plasticized and the membrane is under a constant compaction force in the cell [196]. This may lead to membrane thinning and, eventually, puncturing a pinhole formation. An effect especially pertaining to swelling of the polymer upon water sorption is a fatigue-type phenomenon when the membrane electrode assembly is subjected to dry–wet cycles, which leads to periodic stress build up and relaxation in the membrane and, ultimately, to crack formation. This has been observed to be a membrane failure mode [197].

4.2.7 Fuel Cell Performance

Fuel cell characterization using radiation grafted membranes is mentioned in the work of Sundholm et al. [182, 198–200], Horsfall and Lovell [187, 201], Scott et al. [202], Nasef and Saidi [203], Hatanaka et al. [204], Aricò et al. [183], and Scherer et al. [61, 205–210] (in the last 5 years). In addition, in recent patent literature Ballard Power Systems [97, 211], Aisin Seiki [89, 91], and Pirelli [92] have filed inventions related to radiation grafted fuel cells membranes. The reported fuel cell performance characteristics span a substantial range, from unacceptably poor to values approaching or exceeding comparative samples based on Nafion membranes [43]. It has to be emphasized at this point that direct comparison of fuel cell test data is not always straightforward and can be misleading. Occasionally, the grafted membranes used are thinner than the respective Nafion comparison example. Consequently, similar fuel cell performance can be obtained although the conductivities of the two membrane materials are notably dissimilar. Crosslinked membranes have been used only in the minority of experiments by Nezu et al. [89], Aricò et al. [183], and in our own laboratory, e.g., [207]. The influence of DVB as crosslinker on ex situ membrane properties was discussed earlier. In the fuel cell, the level of crosslinking affects performance as well as durability [208] (also, Gubler et al. unpublished results). Optimum performance was found for 10% DVB content as a consequence of balanced

membrane resistance and membrane-electrode interface characteristics. Stable performance was observed over a few hundred hours only for membranes with 10 and 20% DVB; the lower crosslinked membranes showed significant degradation. Membranes with high crosslinker content of 20% or more, however, suffer from poor mechanical properties. The increasing brittleness of the material can lead to membrane cracking during MEA fabrication or fuel cell operation.

One of the degradation modes observed using radiation grafted fuel cell membranes is correlated with reactant gas (i.e., H_2 and O_2) permeability through the membrane. Kallio et al. [182] found that oxygen diffusion and permeability increase with increasing water uptake and thus with DG. The open circuit voltage of the fuel cell was observed to be lower for membranes with higher water uptake, indicating a higher extent of mixed potential formation, especially on the cathode, due to gas permeation. Similar observations were made by Büchi et al. [125] as lower degrees of crosslinking at similar graft level yield membranes with higher water uptake, higher gas permeation, lower open circuit voltage, and shorter membrane lifetime in the fuel cell.

As an example for MEA performance, Fig. 20 shows the polarization behavior of an optimized radiation grafted membrane on the basis of FEP-25 film with 18% DG and 10% crosslinker content, compared against

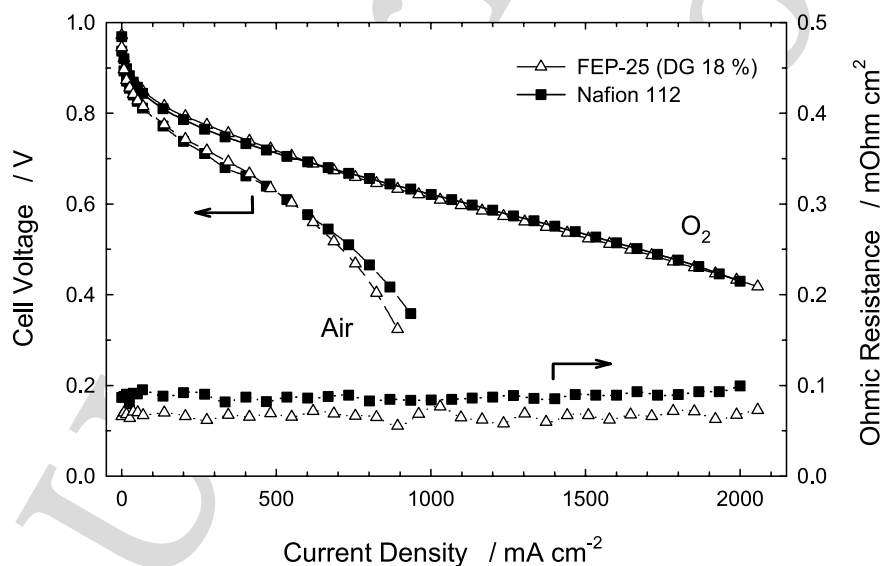


Fig. 20 Single cell performance comparison. Conditions: cell temperature 80 °C, H_2 stoichiometry 1.5, O_2 /air stoichiometry 9.5/2.0, both fuel and oxidant reactant gases fully humidified, ambient pressure. Ohmic resistance was determined using auxiliary fast-current pulses according to [214]

a Nafion 112-based MEA. The polarization curve of the two MEAs is similar, with a slightly lower ohmic resistance of the sample with the grafted membrane, which, however, is offset by a slightly higher interface resistance. This membrane is optimized for performance, durability, and mechanical stability. A membrane of this configuration was operated for over 4000 h at a cell temperature of 80 °C without loss in performance [61].

Very promising fuel cell performance results with respect to longevity were obtained with a novel monomer combination, namely a mixture of α -methylstyrene and methacrylonitrile as graft component [44]. Although these preliminary tests were carried out with non-crosslinked membranes, they nicely show the positive effect of substituting the α -H atom by a methyl group on stability under fuel cell test conditions. Testing of crosslinked membranes is ongoing (Gubler et al. unpublished results).

4.2.8 Performance in Direct Methanol Fuel Cells

The technology of radiation grafting of membranes is particularly interesting for the direct methanol fuel cell (DMFC), because the process parameters can be easily tuned to produce membranes with lower water and methanol

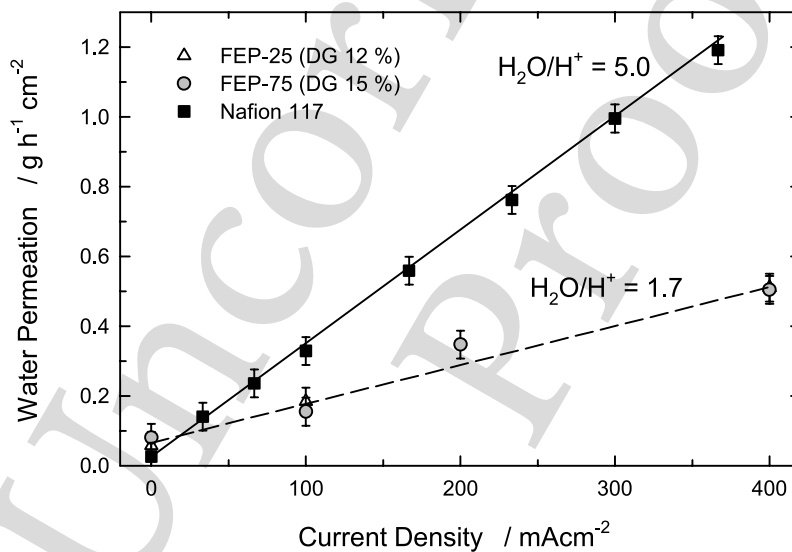


Fig. 21 Water permeation from anode to cathode in the direct methanol fuel cell for radiation grafted membranes based on FEP with different initial film thickness (25 and 75 μm) and Nafion 117. The electroosmotic drag coefficient $\text{H}_2\text{O}/\text{H}^+$ is calculated from the slope of the regression line. Conditions: cell temperature 90 °C, pressure 2 bar, 20 mL min^{-1} , 0.5 M methanol, air stoichiometry is 2.0 for FEP and 3.0 for Nafion 117

uptake, and with the desired transport properties [200,212]. Compared to membranes used in the hydrogen fuel cell, optimized membranes for the DMFC are fabricated using thicker base film such as FEP 75 μm and having a lower DG [209]. With such membranes, identical performance is obtained compared to the Nafion 117 standard, yet with methanol permeation reduced by 40%. In addition, lower water transport from anode to cathode leads to less cathode flooding. Water permeation data from anode to cathode for two radiation grafted membranes based on FEP-25 and FEP-75, and for Nafion 117 are shown in Fig. 21. Water transport through these membranes appears to depend linearly on the cell current with comparably little permeation at zero current, indicating that the dominant mechanism for water transport is electroosmotic drag. From the slope of the curves, the electroosmotic drag coefficient can be calculated, yielding a value of 1.7 for the crosslinked radiation grafted membranes and 5.0 for Nafion 117. Also, the reader may note that there is no marked difference in water permeation between the two grafted membranes of different thickness, reinforcing the conclusion that electroosmotic drag is dominant, and not diffusion.

5 Conclusions

This review demonstrates that radiation grafted membranes can be used successfully as solid polymer electrolytes for fuel cells. The membranes fabricated by radiation-induced grafting offer a cost-competitive option since inexpensive commercial materials are used and the preparation procedure is based on established industrial processes. Radiation-induced grafting is an attractive method to introduce desirable properties into a polymer owing to its simplicity in handling and its control over the grafting process. The method allows the use of a wide range of polymer–monomer combinations, such as various fluoropolymer films and vinyl and acrylic monomers. Partially fluorinated and perfluorinated polymers have been frequently used as base polymer to meet the requirements for chemically and thermally stable proton conducting membranes. Styrene and styrene derivatives have been extensively used as the monomer since grafted styrene can be readily modified to introduce a variety of functionalities.

Grafting parameters (irradiation dose, monomer concentration, grafting medium, temperature, etc.) have significant influence not only on grafting yield and grafting kinetics but also on resultant film and membrane properties. Crosslinkers are used in conjunction with the monomer to achieve certain desirable properties. For instance, the use of crosslinker is an effective means of enhancing the stability of styrene-grafted membranes in fuel cells.

Investigation of the structure, morphology, homogeneity, thermal and mechanical properties of both the grafted films and the membranes is important

for understanding the grafting process and the operation mechanisms of the membranes. Several characterization methods are available to examine these properties.

The identification of membrane properties relevant to fuel cells (ion exchange capacity, water uptake, conductivity), aspects of membrane electrode assembly fabrication, and fuel cell performance are described in detail in this review.

References

1. Bungay PM, Lonsdale HK, Pinho MN (1986) (eds) *Synthetic membranes: science, engineering and applications*. Reidel, Dordrecht
2. Lemmons RJ (1990) *J Power Source* 29:251
3. Doyle M, Rajendran G (2003) Perfluorinated membranes. In: Vielstich W, Gasteiger HA, Lamm A (eds) *Handbook of fuel cells: fundamentals, technology and applications*, vol 3. Wiley, Chichester, p 351
4. Smitha B, Sridhar S, Khan AA (2003) *J Membr Sci* 225:63
5. Vie P, Paronen M, Stromgard M, Rauhala E, Sundholm F (2002) *J Membr Sci* 204:295
6. Paronen M, Sundholm F, Rauhala E, Lehtinen T, Hietala S (1997) *J Mater Chem* 7:2401
7. Kato K, Uchida E, Kang ET, Uyama Y, Ikada Y (2003) *Prog Polym Sci* 28:209
8. Schellekens MAJ, Klumperman B (2000) *J Macromol Sci Rev Macromol Chem Phys C* 40:167
9. Gupta B, Scherer GG (1994) *Chimia* 48:127
10. Hegazy EA, AbdEl-Rehim HA, Kamal H, Kandeel KA (2001) *Nucl Instrum Methods Phys Res B* 185:235
11. Rikukawa M, Sanui K (2000) *Prog Polym Sci* 25:1463
12. Cardona F, George GA, Hill DJT, Perera S (2003) *Polym Int* 52:827
13. Dargaville TR, George GA, Hill DJT, Whittaker AK (2003) *Prog Polym Sci* 28:1355
14. Nasef MM, Hegazy EA (2004) *Prog Polym Sci* 29:499
15. Kabanov VY (2004) *High Energ Chem* 38:57
16. Hickner MA, Ghassemi H, Kim YS, Einsla BR, McGrath JE (2004) *Chem Rev* 104:4587
17. Smitha B, Sridhar S, Khan AA (2005) *J Membr Sci* 259:10
18. Souzy R, Ameduri B (2005) *Prog Polym Sci* 30:644
19. Hickner MA, Pivovar BS (2005) *Fuel Cells* 5:213
20. Jagur-Grodzinski J (2007) *Polym Adv Technol* 18:785
21. Chapiro A (1962) *Radiation chemistry of polymeric systems*. Wiley-Interscience, New York
22. Chapiro A (1977) *Radiat Phys Chem* 9:55
23. Fischer NK, Corelli JC (1981) *J Polym Sci A* 19:2465
24. Lunkwitz K, Brink HJ, Handle D, Ferse A (1989) *Radiat Phys Chem* 33:523
25. Bürger W, Lunkwitz K, Pompe G, Petr A, Jehnichen D (1993) *J Appl Polym Sci* 48:1973
26. Iwasaki M (1971) *Fluorine Chem Rev* 5:1
27. Lappan U, Häussler L, Pompe G, Lunkwitz K (1997) *J Appl Polym Sci* 66:2287
28. Iwasaki M, Toriyama K (1967) *J Chem Phys* 47:559
29. Schlick S, Chamulitrat W, Kevan L (1985) *J Phys Chem* 89:4278
30. Hill DJT, Mohajerani S, Pomeri PJ, Whittaker AK (2000) *Radiat Phys Chem* 59:295

- 2442 31. Dargaville TR, Hill DJT, Whittaker AK (2001) *Radiat Phys Chem* 62:25 2442
- 2443 32. Oshima A, Seguchi T, Tabata Y (1997) *Radiat Phys Chem* 50:601 2443
- 2444 33. Lunkwitz K, Lappan U, Lehmann D (2000) *Radiat Phys Chem* 57:373 2444
- 2445 34. Nasef MM, Dahlan KJM (2003) *Nucl Instrum Methods Phys Res B* 201:604 2445
- 2446 35. Oshima A, Ikeda S, Katoh E, Tabata Y (2001) *Radiat Phys Chem* 62:38 2446
- 2447 36. Tabata Y, Oshima A, Takashika K, Saguchi T (1996) *Radiat Phys Chem* 48:563 2447
- 2448 37. Oshima A, Tabata Y, Kudoh H, Seguchi T (1995) *Radiat Phys Chem* 45:269 2448
- 2449 38. Sun J, Zhang Y, Zhong X (1994) *Polymer* 35:2881 2449
- 2450 39. Zhong X, Sun J, Zhang Y (1992) *Polymer* 33:5341 2450
- 2451 40. Zhong X, Sun J, Wang F, Sun Y (1992) *J Appl Polym Sci* 44:639 2451
- 2452 41. Sun J, Zhang Y, Zhong X, Zhang W (1993) *Radiat Phys Chem* 42:139 2452
- 2453 42. Forsythe JS, Hill DJT, Logothetis AL, Seguchi T, Whittaker AK (1998) *Radiat Phys Chem* 53:611 2453
- 2454 43. Gubler L, Gürsel SA, Scherer GG (2005) *Fuel Cells* 5:317 2454
- 2455 44. Gubler L, Slaski M, Wokaun A, Scherer GG (2006) *Electrochem Commun* 8:1215 2455
- 2456 45. Alkan Gürsel S, Yang Z, Choudhury B, Roelofs MG, Scherer GG (2006) *J Electrochem Soc* 53:A1964 2456
- 2457 46. Chen J, Asano M, Yamaki T, Yoshida M (2006) *J Appl Polym Sci* 100:4565 2457
- 2458 47. Chapiro A (1959) *J Polym Sci* 34:481 2458
- 2459 48. Chapiro A (1962) *J Polym Sci* 57:743 2459
- 2460 49. Chapiro A (1979) *Radiat Phys Chem* 14:101 2460
- 2461 50. Chapiro A (1987) *Eur Polym J* 23:255 2461
- 2462 51. Bozzi A, Chapiro A (1988) *Radiat Phys Chem* 32:193 2462
- 2463 52. Gupta B, Chapiro A (1989) *Eur Polym J* 25:1137 2463
- 2464 53. Gupta B, Chapiro A (1989) *Eur Polym J* 25:1145 2464
- 2465 54. Gupta B, Anjum N (2000) *J Appl Polym Sci* 77:1331 2465
- 2466 55. Phadnis S, Patri M, Hande VR, Deb P (2003) *J Appl Polym Sci* 90:2572 2466
- 2467 56. Cardona F, George GA, Hill DJT, Rasoul F, Maeji J (2002) *Macromolecules* 35:355 2467
- 2468 57. Cardona F, George GA, Hill DJT, Perera S (2002) *J Polym Sci A* 40:3191 2468
- 2469 58. Souzy R, Ameduri B, Boutevin B, Gebel G, Capron P (2005) *Solid State Ionics* 176:2839 2469
- 2470 59. Brack HP, Büchi FN, Huslage J, Scherer GG (1998) *Proc Electrochem Soc* 27:52 2470
- 2471 60. Huslage J, Rager T, Schnyder B, Tsukada A (2002) *Electrochim Acta* 48:247 2471
- 2472 61. Gubler L, Kuhn H, Schmidt TJ, Scherer GG, Brack HP, Simbeck F (2004) *Fuel Cells* 4:196 2472
- 2473 62. Brack HP, Büchi FN, Huslage J, Rota M, Scherer GG (2000) Development of radiation grafted membranes for fuel cell applications based on poly(ethylene-*alt*-tetrafluoroethylene). In: Pinnau I, Freeman BD (eds) *Membrane formation and modification*. ACS symposium series 744. Oxford University Press, New York, p 174 2473
- 2474 63. Brack HP, Scherer GG (1997) *Macromol Symp* 126:25 2474
- 2475 64. Brack HP, Bühner HG, Bonorand L, Scherer GG (2000) *J Mater Chem* 10:1795 2475
- 2476 65. Walsby N, Sundholm F, Kallio T, Sundholm G (2001) *J Polym Sci A* 39:3008 2476
- 2477 66. Lee W, Shibasaki A, Saito K, Sugita K, Okuyama K, Suyo T (1996) *J Electrochem Soc* 143:2795 2477
- 2478 67. Chen J, Asano M, Maekawa Y, Yoshida M (2005) *J Membr Sci* 277:249 2478
- 2479 68. Chen J, Septiani U, Asano M, Maekawa Y, Kubota H, Yoshida M (2007) *J Appl Polym Sci* 103:1966 2479
- 2480 69. Hegazy EA, Ishigaki I, Okamoto J (1981) *J Appl Polym Sci* 26:3117 2480
- 2481 70. Momose T, Yoshioka H, Ishigaki I, Okamoto J (1989) *J Appl Polym Sci* 37:2817 2481
- 2482 71. Stone C, Bonorand LM (2003) WO 03/018654 A1 (Ballard Power Systems Inc) 2482
- 2483 2484 2485 2486 2487 2488 2489 2490 2491 2492

- 2493 72. Gupta B, Büchi FN, Scherer GG (1994) *J Polym Sci A* 32:1931 2493
- 2494 73. Horsfall JA, Lovell KV (2002) *Eur Polym J* 38:1671 2494
- 2495 74. Nasef MM, Saidi H, Dessouki AM, El-Nesr EM (2000) *Polym Int* 49:399 2495
- 2496 75. Nasef MM, Saidi H, Nor HM (2000) *J Appl Polym Sci* 76:220 2496
- 2497 76. Rager T (2003) *Helv Chim Acta* 86:1 2497
- 2498 77. Rager T (2004) *Helv Chim Acta* 87:400 2498
- 2499 78. Nasef MM (2001) *Polym Int* 50:338 2499
- 2500 79. Dargaville TR, George GA, Hill DJT, Whittaker AK (2003) *Macromolecules* 36:8276 2500
- 2501 80. Alkan Gürsel S, Ben youcef H, Wokaun A, Scherer GG (2007) *Nucl Instrum Methods Phys Res B* 265:198 2501
- 2502 81. Rohani R, Nasef MM, Saidi H, Zaman K, Dahlan M (2007) *Chem Eng J* 132:27 2503
- 2503 82. Hegazy EA, Ishigaki I, Dessouki AM, Rabie A-GM, Okamoto J (1982) *J Appl Polym Sci* 27:535 2504
- 2504 83. Phadnis S, Patri M, Hande VR, Deb PC (2003) *J Appl Polym Sci* 90:2572 2505
- 2505 84. Septiani U, Chen J, Asano M, Maekawa Y, Yoshida M, Kubota H (2007) *J Mater Sci* 42:1330 2506
- 2506 85. Liang GZ, Lu TL, Ma XY, Yan HX, Gong ZH (2003) *Polym Int* 52:1300 2507
- 2507 86. Nasef MM, Saidi H, Nor HM, Dahlan KZM, Hashim K (1999) *J Appl Polym Sci* 73:2095 2508
- 2508 87. Elmidaoui A, Cherif AT, Brunea J, Duclert F, Cohen T, Gavach C (1992) *J Membr Sci* 67:263 2509
- 2509 88. Becker W, Bothe M, Schmidt-Naake G (1999) *Angew Makromol Chem* 273:57 2510
- 2510 89. Nezu S, Ito N, Yamada C, Kato M, Asukabe M (2001) US Patent 6 242 123 (Aisin Seiki Kabushiki Kaisha) 2511
- 2511 90. D'Agostino VF, Newton JM (2001) US Patent 6 225 368 (National Power PLC) 2512
- 2512 91. Asukabe M, Kato M, Taniguchi T, Morimoto Y, Kawasumi M (2004) US Patent US 6 827 986 B2 (Aisin Seiki Kabushiki Kaisha) 2513
- 2513 92. Dubitsky YA, Lopes Correia Tavares AB, Zaopo A, Albizzati E (2004) WO 2004/004053 A2 (Pirelli & C. SpA) 2514
- 2514 93. D'Agostino VF, Lee JY, Cook EH (1977) US Patent 4 012 303 (Hooker Chemicals & Plastics Corp) 2515
- 2515 94. D'Agostino VF, Lee JY, Cook EH (1978) US Patent 4 107 005 (Hooker Chemicals & Plastics Corp) 2516
- 2516 95. D'Agostino VF, Lee JY, Cook EH (1978) US Patent 4 113 922 (Hooker Chemicals & Plastics Corp) 2517
- 2517 96. Momose T, Tomiie K, Harada H, Miyachi H, Kato H (1986) US Patent 4 605 685 (Chlorine Engineers Corp) 2518
- 2518 97. Stone C, Steck AE (2002) US Patent US 6 359 019 (Ballard Power Systems Inc) 2519
- 2519 98. MacKinnon SM (2004) US Patent 6 828 386 (Ballard Power Systems Inc) 2520
- 2520 99. Sean MM (2004) US Patent 2004/0059015 A1 (Ballard Power Systems Inc) 2521
- 2521 100. Stone C, Steck AE, Choudhury B (2002) US Patent US 2002/0137806 A1 (Ballard Power Systems Inc) 2522
- 2522 101. Stone C (2003) WO 03/018655 A1 (Ballard Power Systems Inc) 2523
- 2523 102. Stone C, Steck AE (2001) WO 01/58576 A1 (Ballard Power Systems Inc) 2524
- 2524 103. Yang Z, Roelofs MG, Alkan Gürsel S, Scherer GG (2006) IP WO 2006/102672 2525
- 2525 104. Slaski M, Gubler L, Scherer GG (2006) EPA WO 2006/084591 A1 2526
- 2526 105. Momose T, Tomiie K, Ishigaki I, Okamoto J (1989) *J Appl Polym Sci* 37:2165 2527
- 2527 106. Dargaville TR, Hill DJT, Perera S (2002) *Aust J Chem* 55:439 2528
- 2528 107. Walsby N, Paronen M, Juhanoja J, Sundholm F (2000) *J Polym Sci A* 38:1512 2529
- 2529 2530 2531 2532 2533 2534 2535 2536 2537 2538 2539 2540 2541 2542 2543

- 2544 108. Brandrup J, Immergut EH (1989) *Polymer Handbook*. Wiley-Interscience, New York, 2544
p 519 2545
- 2546 109. Farquet P, Kunze A, Padeste C, Solak HH, Alkan Gürsel S, Scherer GG, Wokaun A 2546
(2007) *Polymer* 48:4936 2547
- 2548 110. Odian G (1970) *Principles of polymerization*. McGraw-Hill, New York, p 255 2548
- 2549 111. Walsby N, Paronen M, Juhanoja J, Sundholm F (2001) *J Appl Polym Sci* 81:1572 2549
- 2550 112. Hegazy EA, Taher NH, Kamal H (1989) *J Appl Polym Sci* 38:1229 2550
- 2551 113. El-Assy N (1991) *J Appl Polym Sci* 42:885 2551
- 2552 114. Gupta B, Scherer GG (1993) *Angew Makromol Chem* 210:151 2552
- 2553 115. Nasef MM, Saidi H (2003) *J Membr Sci* 216:27 2553
- 2554 116. Gupta B, Büchi FN, Scherer GG, Chapiro A (1996) *J Membr Sci* 118:231 2554
- 2555 117. Chen J, Asano M, Yamaki T, Yoshida M (2006) *J Appl Polym Sci* 100:4565 2555
- 2556 118. Ben youcef H, Alkan Gürsel S, Wokaun A, Scherer GG (2008) *J Membr Sci* 311:208 2556
- 2557 119. Becker W, Schmidt-Naake G (2002) *Chem Eng Technol* 25:4 2557
- 2558 120. Rota M, Brack HP, Büchi FN, Gupta B, Haas O, Scherer GG (1995) Extended abstracts 2558
of 187th meeting of the Electrochemical Society, Reno, NV, 21–26 May 1995. 95-1:719 2559
- 2560 121. Büchi FN, Gupta B, Haas O, Scherer GG (1995) *J Electrochem Soc* 142:3044 2560
- 2561 122. Brack HP, Scherer GG (1998) Abstracts of papers of the American Chemical Society 2561
216:281 – PMSE Part 2 2562
- 2563 123. Steuernagel L, Reich S, Kaufmann DE, Wokaun A, Scherer GG, Brack HP (2002) PSI 2563
scientific report. Villigen PSI, Switzerland, p 25^{CE^a} 2564
- 2565 124. Brack HP, Fischer D, Peter G, Slaski M, Scherer GG (2004) *J Polym Sci A* 42:59 2565
- 2566 125. Büchi FN, Gupta B, Haas O, Scherer GG (1995) *Electrochim Acta* 40:345 2566
- 2567 126. Rouilly MV, Kötz, Haas O, Scherer GG, Chapiro A (1993) *J Membr Sci* 81:89 2567
- 2568 127. Gupta B, Büchi FN, Staub M, Grman D, Scherer GG (1996) *J Polym Sci A* 34:1873 2568
- 2569 128. Yamaki T, Asano M, Maekawa Y, Morita Y, Suwa T, Chen J, Tsubokawa N, Kobayashi K, 2569
Kubota H, Yoshida M (2003) *Radiat Phys Chem* 67:403 2570
- 2571 129. Gupta B, Anjum N (2001) *J Appl Polym Sci* 82:2629 2571
- 2572 130. Sakurai H, Shiotani M, Yahiro H (1999) *Radiat Phys Chem* 56:309 2572
- 2573 131. Oshima A, Tabata Y, Kudoh H, Seguchi T (1995) *Radiat Phys Chem* 45:269 2573
- 2574 132. Sato K, Ikeda S, Iida M, Oshima A, Tabata Y, Washio M (2003) *Nucl Instrum Methods* 2574
Phys Res B 208:424 2575
- 2576 133. Nasef MM, Saidi H, Nor HM (2000) *J Appl Polym Sci* 77:1877 2576
- 2577 134. Flint SD, Slade RCT (1997) *Solid State Ionics* 97:299 2577
- 2578 135. Gupta B, Büchi FN, Scherer GG, Chapiro A (1994) *Polym Adv Technol* 5:493 2578
- 2579 136. Alkan Gürsel S, Yang Z, Choudhury B, Roelofs MG, Scherer GG (2006) *J Electrochem* 2579
Soc 53:A1964 2580
- 2581 137. Mattsson B, Ericson H, Torell LM, Sundholm F (1999) *J Polym Sci A* 37:3317 2581
- 2582 138. Gupta B, Staub M, Scherer GG, Grman D (1995) *J Polym Sci A* 33:1545 2582
- 2583 139. Schnyder B, Rager T (2007) *J Appl Polym Sci* 104:1973 2583
- 2584 140. Hietala S, Paronen M, Holmberg S, Nasman J, Juhanoja J, Karjalainen M, Serimaa R, 2584
Toivola M, Lehtinen T, Parovuori K, Sundholm G, Ericson H, Mattsson B, Torell L, 2585
Sundholm F (1999) *J Polym Sci A* 37:1741 2586
- 2587 141. Hegazy EA, Ishigaki I, Rabie A-GM, Dessouki AM, Okamoto J (1983) *J Appl Polym* 2587
Sci 28:1465 2588
- 2589 142. Hegazy EA, Ishigaki I, Rabie A-GM, Dessouki AM, Okamoto J (1981) *J Appl Polym* 2589
Sci 26:3871 2590
- 2591 143. Guilmeau I, Esnouf S, Betz N, Le Moel A (1997) *Nucl Instrum Methods Phys Res B* 2591
131:270 2592
- 2593 2593
- 2594 2594

DOI: 10.1007/12_2008_153

Date: 2008-05-21

Proof-Number: 1

^{CE^a} Dear author, if this is available online, please give web address

- 2595 144. Ericson H, Kallio T, Lehtinen T, Mattsson B, Sundholm G, Sundholm F, Jacobsson P 2595
2596 (2002) *J Electrochem Soc* 149:A206 2596
2597 145. Mattsson B, Ericson H, Torell LM, Sundholm F (2000) *Electrochim Acta* 45:1405 2597
2598 146. Brack HP, Büchi FN, Huslage J, Scherer GG (1998) In: Gottesfeld S, Fuller TF (eds) 2598
2599 Proton conducting membrane fuel cells II. *Electrochemical Society PV* 98-27:52 2599
2600 147. Good RJ (1992) *J Adhes Sci Technol* 6:1269 2600
2601 148. Gupta B, Anjum N (2002) *J Appl Polym Sci* 86:1118 2601
2602 149. Brack HP, Wyler M, Peter G, Scherer GG (2003) *J Membr Sci* 214:1 2602
2603 150. Brack HP, Slaski M, Gubler L, Scherer GG, Alkan Gürsel S, Wokaun A (2004) *Fuel* 2603
2604 *Cells* 4:1 2604
2605 151. Nasef MM, Saidi H, Nor HM, Yarmo MA (2000) *J Appl Polym Sci* 76:336 2605
2606 152. Nasef MM, Saidi H (2006) *Appl Surf Sci* 252:3073 2606
2607 153. Gebel G, Ottomani E, Allegraud JJ, Betz N, Le Moel A (1995) *Nucl Instrum Methods* 2607
2608 *Phys Res B* 105:145 2608
2609 154. Gebel G, Diat O (2005) *Fuel Cells* 5:261 2609
2610 155. Hietala S, Holmberg S, Näsman J, Ostrovskii Paronen M, Serimaa R, Sundholm F, 2610
2611 Torell L, Torkkeli M (1997) *Angew Makromol Chem* 253:151 2611
2612 156. Jokela K, Galambosi S, Karjalainen M, Torkkeli M, Serimaa R, Eteläniemi V, Vah- 2612
2613 vasselkä S, Hietala S, Paronen M, Sundholm F (2000) *Mater Sci Forum* 321–324:481 2613
2614 157. Elomaa M, Hietala S, Paronen M, Walsby N, Jokela K, Serimaa R, Torkkeli M, Lehti- 2614
2615 nen T, Sundholm G, Sundholm F (2000) *J Mater Chem* 10:2678^{CE^b} 2615
2616 158. Aymes-Chodur C, Betz N, Porte-Durrieu MC, Baquey C, Le Moel A (1999) *Nucl* 2616
2617 *Instrum Methods Phys Res B* 151:377 2617
2618 159. Gupta B, Scherer GG (1993) *J Appl Polym Sci* 50:2129 2618
2619 160. Gupta B, Highfield JG, Scherer GG (1994) *J Appl Polym Sci* 51:1659 2619
2620 161. Brack HP, Rüegg D, Bühler H, Slaski M, Alkan Gürsel S, Scherer GG (2004) *J Polym* 2620
2621 *Sci B Polym Phys* 42:2612 2621
2622 162. Alkan Gürsel S, Schneider J, Ben Youcef H, Wokaun A, Scherer GG (2008) *J Appl* 2622
2623 *Polym Sci* 108:3577 2623
2624 163. Cardona F, Hill DJT, George GA, Maeji J, Firas R, Perera S (2001) *Polym Degrad* 2624
2625 *Stabil* 74:219 2625
2626 164. Hietala S, Koel M, Skou E, Elomaa M, Sundholm F (1998) *J Mater Chem* 8:1127 2626
2627 165. Nasef MM, Saidi H, Nor HM, Foo OM (2000) *J Appl Polym Sci* 78:2443 2627
2628 166. Gupta B, Haas O, Scherer GG (1994) *J Appl Polym Sci* 54:469 2628
2629 167. Zevin L, Messalem R (1982) *Polymer* 23:601 2629
2630 168. Nasef MM, Saidi H (2006) *Macromol Mater Eng* 291:972 2630
2631 169. Nasef MM (2002) *Eur Polym J* 38:87 2631
2632 170. Jokela K, Serimaa R, Torkkeli M, Sundholm F, Kallio T, Sundholm G (2002) *J Polym* 2632
2633 *Sci A* 40:1539 2633
2634 171. Gupta B, Scherer GG, Highfield J (1998) *Angew Makromol Chem* 256:81 2634
2635 172. Scherer GG, Brack HP, Büchi FN, Gupta B, Haas O, Rota M (1996) Hydrogen energy 2635
2636 progress XI. Proceedings of the 11th world hydrogen energy conference, Stuttgart, 2636
2637 Germany. 2:1727 2637
2638 173. Scherer GG (1990) *Ber Bunsenges Phys Chem* 94:1008 2638
2639 174. He R, Li Q, Xiao G, Bjerrum NJ (2003) *J Membr Sci* 226:169 2639
2640 175. Taniguchi T, Morimoto T, Kawakado M (2001) JP 2001/213987A2 (Toyota Central 2640
2641 Research & Development Laboratory Inc) 2641
2642 176. Nasef MM, Saidi H, Nor HM, Foo OM (2000) *J Appl Polym Sci* 76:1 2642
2643 177. Lehtinen T, Sundholm G, Holmberg S, Sundholm F, Björnbohm B, Bursell M (1998) 2643
2644 *Electrochim Acta* 43:1881 2644
2645

DOI: 10.1007/12_2008_153

Date: 2008-05-21

Proof-Number: 1

^{CE^b} Please note that Mortensen et al., submitted, has been deleted from the list and moved to the text

- 2646 178. Kreuer KD (2001) *J Membr Sci* 185:29 2646
- 2647 179. Choi P, Jalani NH, Datta R (2005) *J Electrochem Soc* 152:E123 2647
- 2648 180. Halim J, Büchi FN, Haas O, Stamm M, Scherer GG (1994) *Electrochim Acta* 39:1303 2648
- 2649 181. Kreuer KD (1992) In: Colombari P (ed) *Proton conductors*. Cambridge University 2649
- 2650 Press, Cambridge, p 474 2650
- 2651 182. Kallio T, Lundström M, Sundholm G, Walsby N, Sundholm F (2002) *J Electrochem* 2651
- 2652 32:11 2652
- 2653 183. Aricò AS, Baglio V, Cretì P, Blasi AD, Antonucci V, Brunea J, Chapotot A, Bozzi A, 2653
- 2654 Schoemans J (2003) *J Power Source* 123:107 2654
- 2655 184. Gubler L, Finsterwald T, Keller M, Scherer GG (2005) International conference on 2655
- 2656 solid state ionics, SSI 15, Baden-Baden, Germany, 17–22 July 2005. Oral contribution 2656
- 2657 no 78 2657
- 2658 185. Walsby N, Hietala S, Maunu SL, Sundholm F, Kallio T, Sundholm G (2002) *J Appl* 2658
- 2659 *Polym Sci* 86:33 2659
- 2660 186. Kreuer KD (1997) *Solid State Ionics* 97:1 2660
- 2661 187. Horsfall JA, Lovell KV (2001) *Fuel Cells* 13:186 2661
- 2662 188. Gupta B, Haas O, Scherer GG (1995) *J Appl Polym Sci* 57:855 2662
- 2663 189. Jiang R, Chu D (2004) *J Electrochem Soc* 151:A69 2663
- 2664 190. LaConti AB, Hamdan H, McDonald RC (2003) Mechanisms of membrane degrada- 2664
- 2665 tion. In: Vielstich W, Lamm A, Gasteiger H (eds) *Handbook of fuel cells: fundamen-* 2665
- 2666 *tals, technology, applications, vol 3*. Wiley, Chichester, p 647 2666
- 2667 191. Chen J, Asano M, Yamaki T, Yoshida M (2006) *J Mater Sci* 41:1289 2667
- 2668 192. Yamaki T, Tsukada J, Asano M, Katakai R, Yoshida M (2007) *J Fuel Cell Sci Technol* 2668
- 2669 4:56 2669
- 2670 193. Chen J, Septiani U, Asano M, Maekawa Y, Kubota H, Yoshida M (2007) *J Appl Polym* 2670
- 2671 *Sci* 103:1966 2671
- 2672 194. Mitov S, Vogel B, Roduner E, Zhang H, Zhu X, Gogel V, Jörissen L, Hein M, Xing D, 2672
- 2673 Schönberger F, Kerres J (2006) *Fuel Cells* 06:413 2673
- 2674 195. Gubler L, Scherer GG (2008) Durability of radiation grafted fuel cell membranes. In: 2674
- 2675 Inaba M, Schmidt TJ, Büchi FN (eds) *Proton exchange fuel cells durability*. Springer, 2675
- 2676 New York (in press) 2676
- 2677 196. Makharia R, Kocha SS, Yu PT, Gittleman C, Miller D, Lewis C, Wagner RT, Gastei- 2677
- 2678 ger HA (2006) Abstracts of the 208th meeting of the Electrochemical Society, Los 2678
- 2679 Angeles, 16–21 Oct 2005. 502:1165 2679
- 2680 197. Gasteiger HA (2005) International conference on solid state ionics, SSI-15, Baden- 2680
- 2681 Baden, Germany, 17–22 July 2005. Oral contribution no 72 2681
- 2682 198. Gode P, Ihonen J, Strandroth A, Ericson H, Lindbergh G, Paronen M, Sundholm F, 2682
- 2683 Sundholm G, Walsby N (2003) *Fuel Cells* 3:21 2683
- 2684 199. Kallio T, Kisko K, Kontturi K, Serimaa R, Sundholm F, Sundholm G (2004) *Fuel Cells* 2684
- 2685 4:328 2685
- 2686 200. Saarinen V, Kallio T, Paronen M, Tikkanen P, Rauhala E, Kontturi K (2005) *Elec-* 2686
- 2687 *trochim Acta* 50:3453 2687
- 2688 201. Horsfall JA, Lovell KV (2002) *Polym Adv Technol* 13:381 2688
- 2689 202. Scott K, Taama WM, Argyropoulos P (2000) *J Membr Sci* 171:119 2689
- 2690 203. Nasef MM, Saidi H (2002) *J New Mater Electrochem Syst* 5:183 2690
- 2691 204. Hatanaka T, Hasegawa N, Kamiya A, Kawasumi M, Morimoto Y, Kawahara K (2002) 2691
- 2692 *Fuel* 81:2173 2692
- 2693 205. Huslage J, Rager T, Kiefer J, Steuernagel L, Scherer GG (2000) Proceedings of 197th 2693
- 2694 Electrochemical Society Meeting, Toronto, Canada. 14–18 May 2000. 2694
- 2695 2695
- 2696 2696

- 2697 206. Geiger AB, Rager T, Matejcek L, Scherer GG, Wokaun A (2001) In: Büchi FN, 2697
2698 Scherer GG, Wokaun A (eds) Proceedings of 1st European PEFC Forum. Lucerne, 2698
2699 Switzerland, 2–6 July 2001. p 124 2699
- 2700 207. Gubler L, Beck N, Gürsel SA, Hajbolouri F, Kramer D, Reiner A, Steiger B, Scherer GG, 2700
2701 Wokaun A, Rajesh B, Thampi KR (2004) Chimia 58:826 2701
- 2702 208. Schmidt TJ, Simbeck K, Scherer GG (2005) J Electrochem Soc 152:A93 2702
- 2703 209. Gubler L, Gürsel SA, Slaski M, Geiger F, Scherer GG, Wokaun A (2005) Proceedings 2703
2704 of 3rd European PEFC Forum, Lucerne, Switzerland, 4–8 July 2005. Oral presenta- 2704
2705 tion B113 2705
- 2706 210. Gubler L, Prost N, Alkan Gürsel S, Scherer GG (2005) Solid State Ionics 176:2849 2706
2707 ^{CE^c} 2707
- 2708 211. Stone C, Steck AE, Choudhury B (2004) US Patent 6 723 758 (Ballard Power Systems 2708
2709 Inc) 2709
2710 ^{CE^d} 2710
- 2711 212. Geiger AB, Rager T, Huslage J, Scherer GG, Wokaun A (2001) PSI scientific report, 2711
2712 vol 5. Villigen PSI, Switzerland, p 99^{CE^e} 2712
- 2713 213. Chuy C, Basura VI, Simon E, Holdcroft S, Horsfall J, Lovell KV (2000) J Electrochem 2713
2714 Soc 147:4453 2714
- 2715 214. Büchi FN, Marek A, Scherer GG (1995) J Electrochem Soc 142:1895 2715
2716 2716
2717 2717
2718 2718
2719 2719
2720 2720
2721 2721
2722 2722
2723 2723
2724 2724
2725 2725
2726 2726
2727 2727
2728 2728
2729 2729
2730 2730
2731 2731
2732 2732
2733 2733
2734 2734
2735 2735
2736 2736
2737 2737
2738 2738
2739 2739
2740 2740

DOI: 10.1007/12_2008_153

Date: 2008-05-21

Proof-Number: 1

^{CE^c} Please note that Gubler et al., submitted, has been deleted from the list and moved to the text

^{CE^d} Please note that Gubler et al., to be published, has been deleted from the list and moved to the text

^{CE^e} Dear author, if this is available online, please give web address